Biogeosciences, 11, 709–734, 2014
www.biogeosciences.net/11/709/2014/
doi:10.5194/bg-11-709-2014

Biogeosciences Open Access

Air–sea CO_2 flux in the Pacific Ocean for the period 1990–2009

M. Ishii[1,2], R. A. Feely[3], K. B. Rodgers[4], G.-H. Park[5,6,*], R. Wanninkhof[5], D. Sasano[1,2], H. Sugimoto[2], C. E. Cosca[3], S. Nakaoka[7], M. Telszewski[7,], Y. Nojiri[7], S. E. Mikaloff Fletcher[8], Y. Niwa[1], P. K. Patra[9], V. Valsala[7,***], H. Nakano[1], I. Lima[10], S. C. Doney[10], E. T. Buitenhuis[11], O. Aumont[12], J. P. Dunne[13], A. Lenton[14], and T. Takahashi[15]**

[1]Oceanography and Geochemistry Research Department, Meteorological Research Institute, Japan Meteorological Agency, Tsukuba, 305-0052, Japan
[2]Global Environment and Marine Department, Japan Meteorological Agency, Tokyo, 100-8122, Japan
[3]Ocean Climate Research Division, Pacific Marine Environmental Laboratory, NOAA, Seattle, WA 98115, USA
[4]Program in Atmospheric and Oceanic Sciences, Princeton University, Princeton, NJ 08544, USA
[5]Ocean Chemistry Division, Atlantic Oceanographic and Meteorological Laboratory, NOAA, Miami, FL 33149, USA
[6]Cooperative Institute for Marine and Atmospheric Studies, University of Miami, Miami, FL 33149-1098, USA
[7]Center for Global Environmental Research, National Institute for Environmental Studies, Tsukuba, 305-8506, Japan
[8]National Institute of Water and Atmospheric Research, Wellington, 6021, New Zealand
[9]Research Institute for Global Change, Japan Agency for Marine Science and Technology, Yokohama, 236-0001 Japan
[10]Marine Chemistry and Geochemistry Department, Woods Hole Oceanographic Institution, Woods Hole, MA 02543, USA
[11]School of Environmental Sciences, University of East Anglia, Norwich NR4 7TJ, UK
[12]Laboratoire de Physique des Océans, Centre IRD de Bretagne, 29280 Plouzané, France
[13]Geophysical Fluid Dynamics Laboratory, NOAA, Princeton, NJ, 08540-6649, USA
[14]Centre for Australian Weather and Climate Research, CSIRO Marine and Atmospheric Research, Hobart, Tasmania, 7000, Australia
[15]Lamont-Doherty Earth Observatory, Columbia University, Palisades, NY 10964, USA
[*]now at: East Sea Research Institute, Korea Institute of Ocean Science & Technology, Uljin, 767-813 Korea
[**]now at: International Ocean Carbon Coordination Project, Institute of Oceanology of Polish Academy of Sciences, ul. Powstancow Warszawy, 81-712 Sopot, Poland
[***]now at: Indian Institute of Tropical Meteorology, Pune, Maharashtra, India

Correspondence to: M. Ishii (mishii@mri-jma.go.jp)

Received: 18 June 2013 – Published in Biogeosciences Discuss.: 19 July 2013
Revised: 17 December 2013 – Accepted: 17 December 2013 – Published: 6 February 2014

Abstract. Air–sea CO_2 fluxes over the Pacific Ocean are known to be characterized by coherent large-scale structures that reflect not only ocean subduction and upwelling patterns, but also the combined effects of wind-driven gas exchange and biology. On the largest scales, a large net CO_2 influx into the extratropics is associated with a robust seasonal cycle, and a large net CO_2 efflux from the tropics is associated with substantial interannual variability. In this work, we have synthesized estimates of the net air–sea CO_2 flux from a variety of products, drawing upon a variety of approaches in three sub-basins of the Pacific Ocean, i.e., the North Pacific extratropics (18–66° N), the tropical Pacific (18° S–18° N), and the South Pacific extratropics (44.5–18° S). These approaches include those based on the measurements of CO_2 partial pressure in surface seawater (pCO_2sw), inversions of ocean-interior CO_2 data, forward ocean biogeochemistry models embedded in the ocean general circulation models (OBGCMs), a model with assimilation of pCO_2sw data, and inversions of atmospheric CO_2 measurements. Long-term means, interannual variations and mean seasonal variations of the regionally integrated fluxes were compared in each of the sub-basins over the last two decades, spanning the period from 1990 through 2009. A simple average of the long-term mean fluxes obtained with surface water pCO_2 diagnostics and those obtained with ocean-interior CO_2 inversions are -0.47 ± 0.13 Pg C yr^{-1} in

the North Pacific extratropics, $+0.44 \pm 0.14$ Pg C yr^{-1} in the tropical Pacific, and -0.37 ± 0.08 Pg C yr^{-1} in the South Pacific extratropics, where positive fluxes are into the atmosphere. This suggests that approximately half of the CO_2 taken up over the North and South Pacific extratropics is released back to the atmosphere from the tropical Pacific. These estimates of the regional fluxes are also supported by the estimates from OBGCMs after adding the riverine CO_2 flux, i.e., -0.49 ± 0.02 Pg C yr^{-1} in the North Pacific extratropics, $+0.41 \pm 0.05$ Pg C yr^{-1} in the tropical Pacific, and -0.39 ± 0.11 Pg C yr^{-1} in the South Pacific extratropics. The estimates from the atmospheric CO_2 inversions show large variations amongst different inversion systems, but their median fluxes are consistent with the estimates from climatological pCO$_2$sw data and pCO$_2$sw diagnostics. In the South Pacific extratropics, where CO_2 variations in the surface and ocean interior are severely undersampled, the difference in the air–sea CO_2 flux estimates between the diagnostic models and ocean-interior CO_2 inversions is larger (0.18 Pg C yr^{-1}). The range of estimates from forward OBGCMs is also large (-0.19 to -0.72 Pg C yr^{-1}). Regarding interannual variability of air–sea CO_2 fluxes, positive and negative anomalies are evident in the tropical Pacific during the cold and warm events of the El Niño–Southern Oscillation in the estimates from pCO$_2$sw diagnostic models and from OBGCMs. They are consistent in phase with the Southern Oscillation Index, but the peak-to-peak amplitudes tend to be higher in OBGCMs (0.40 ± 0.09 Pg C yr^{-1}) than in the diagnostic models (0.27 ± 0.07 Pg C yr^{-1}).

1 Introduction

The Pacific Ocean plays an important role in the climate system as a large sink for anthropogenic carbon dioxide (CO_2), and, thereby partially mitigates the large-scale effects of human CO_2 emissions into the atmosphere. Estimates of the net air–sea CO_2 flux based on measurements of partial pressure of CO_2 in near-surface seawater (pCO$_2$sw) and in the marine boundary air show that the extratropics in the North and South Pacific are major oceanic sinks of atmospheric CO_2. Although the CO_2 uptake in these sub-basins is counteracted in part by the large CO_2 outgassing from the tropical zone, the integrated CO_2 uptake by the Pacific Ocean likely accounts for approximately one-third of the global oceanic CO_2 uptake (Takahashi et al., 2009a; Wanninkhof et al., 2013). In addition, it is well recognized that CO_2 outgassing from the tropical Pacific exhibits large variations with the El Niño–Southern Oscillation (ENSO). This large interannual variability in air–sea CO_2 fluxes within the tropical Pacific is thought to play a dominant role in the interannual variability in the global oceanic CO_2 uptake (e.g., Feely et al., 1999, 2002, 2006; Ishii et al., 2004; Takahashi et al., 2009a; Wanninkhof et al., 2013).

However, it is still difficult to quantify the net air–sea CO_2 fluxes from pCO$_2$sw measurements alone. This is primarily because measurements are sparse in both space and time in many parts of the ocean, particularly in the Southern Hemisphere, and because air–sea CO_2 fluxes are not themselves directly measured but are derived and are associated with large uncertainties. Therefore, it is useful to compare the observational results with simulations from ocean models and estimates based on a combination of carbon data and models for the purpose of assessing fluxes over large temporal and spatial scales. Even then, there has been relatively poor agreement between the various approaches for estimating net air–sea CO_2 fluxes in the Pacific Ocean (McKinley et al., 2004; Peylin et al., 2005).

In this work, we begin with a review of what is known about air–sea CO_2 fluxes over the sub-basins of the Pacific Ocean. We then present a synthesis of state-of-the-art assessments of net air–sea CO_2 flux over the past two decades spanning the years from 1990 through 2009. This effort brings together CO_2 flux estimates from a wide range of available approaches: a synthesized climatological pCO$_2$sw data set, diagnostic models that use empirical interpolation schemes applied to the data of pCO$_2$sw, oceanic inversion methods from measurements of ocean-interior dissolved inorganic carbon (DIC) and ocean circulation models, prognostic ocean general ocean circulation models coupled with biogeochemical models (OBGCMs), a data-assimilation model with pCO$_2$sw, and atmospheric CO_2 inversion systems with measurements of atmospheric CO_2 mixing ratio and atmospheric transport models. The goal of this paper is to perform a consistent analysis for these available methods and to arrive at consensus estimates of regionally integrated air–sea CO_2 fluxes for each of the sub-basins of the Pacific Ocean with corresponding estimates of the associated uncertainties. In evaluating the different estimates of CO_2 flux variability, it is important to devote particular attention to the differences in how air–sea CO_2 fluxes vary over different timescales. We begin with a consideration of the time-averaged fluxes over the period from 1990 through 2009. We then consider the interannual and seasonal variability for the same period. This allows us to assess whether community efforts are converging. Finally, we seek to identify the factors that cause the differences in the estimate of the flux among the methods, so that the results presented here can serve to guide future research.

2 Overview of air–sea CO_2 flux in the Pacific Ocean

2.1 Tropical Pacific

The physical and biogeochemical properties in the surface layer of the tropical Pacific show a large contrast between the domains of the western "warm pool" and the eastern "cold tongue" (Figs. 1 and 2). The warm pool is characterized

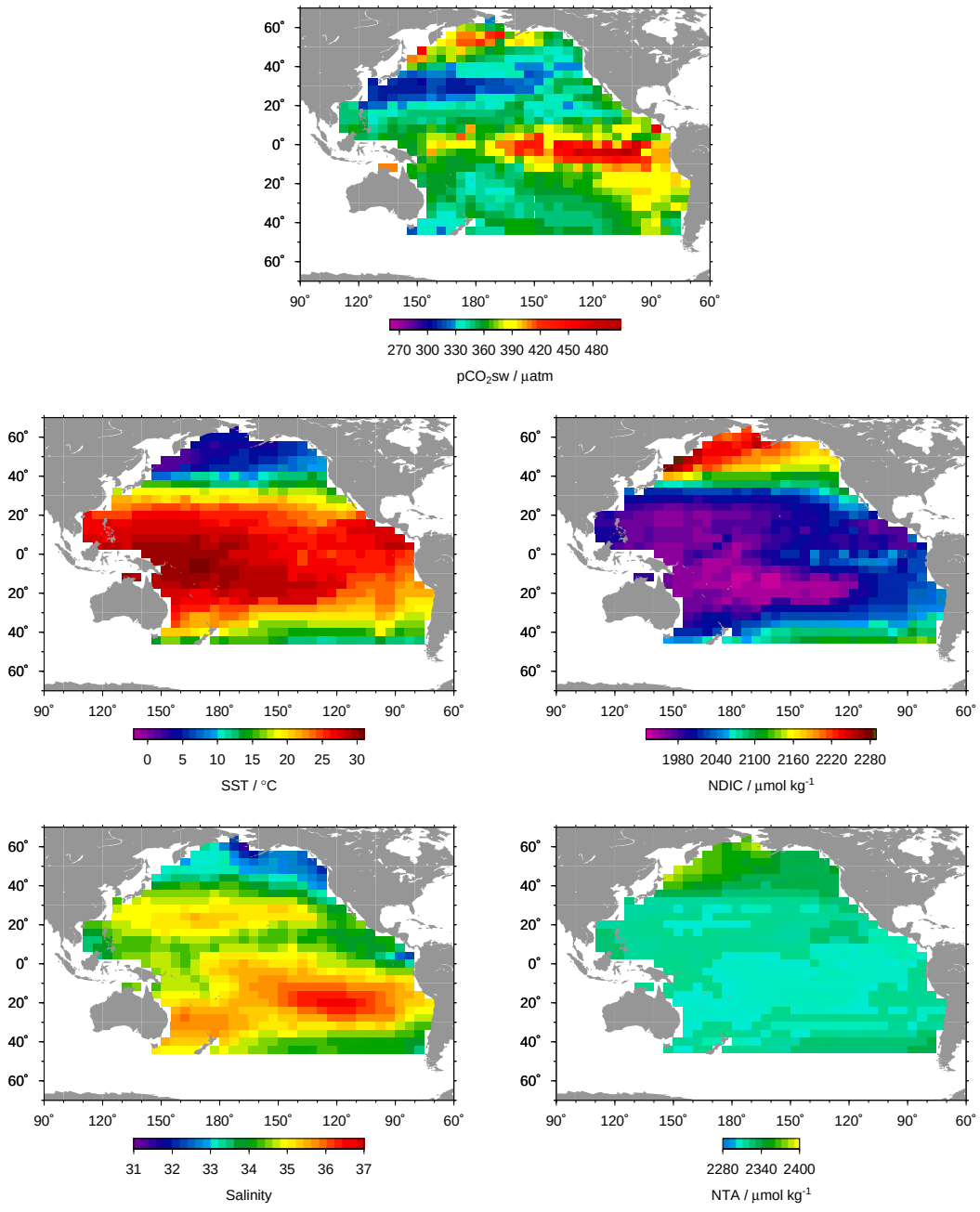

Fig. 1. Data-based climatology in February of pCO_2sw (top panel), temperature (middle left), salinity (bottom left) from LDEO V2009 (Takahashi et al., 2009a), and salinity-normalized ($S = 35$) DIC (middle right) calculated with total alkalinity derived from Lee et al. (2006) (bottom right).

by high sea surface temperatures (SST $> 29.5\,^{\circ}$C) and low sea surface salinities (SSS < 34.8) due to the large solar heat influx and high annual precipitation. As a result of the stratification thus attained, nitrate is depleted and the concentration of DIC is low ($< 1950\,\mu$mol kg^{-1} when salinity-normalized at $S = 35$) in the surface layer of this region. Due to the near equilibration of surface water pCO_2 with atmospheric CO_2, and the presence of low wind speeds, net air–sea CO_2 fluxes over the "warm pool" are relatively small (< 1 mmol m^{-2} day^{-1}; e.g., Ishii and Inoue, 1995).

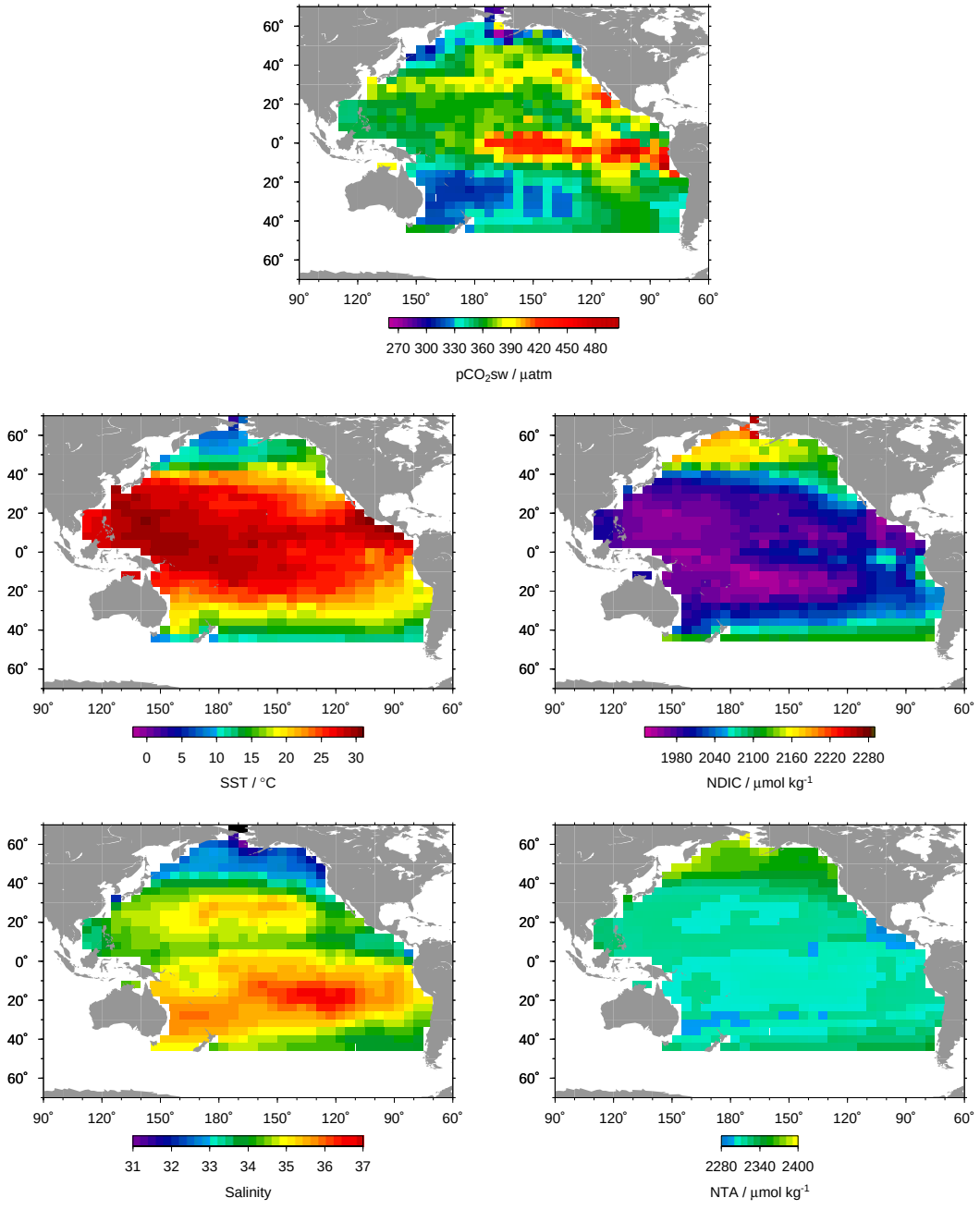

Fig. 2. Same as Fig. 1 but in August.

By contrast, surface water in the eastern tropical Pacific cold tongue region tends to be highly supersaturated with respect to atmospheric CO_2. This is associated with the wind-driven equatorial divergence and turbulent mixing that brings colder, saline and nutrient- and CO_2-rich subsurface waters to the surface. The cold tongue is characterized by lower SSTs ($22 < T\,(°C) < 29$), higher SSSs (> 35), and higher DIC concentrations ($> 1980\,\mu mol\,kg^{-1}$ at $S = 35$) than in the western Pacific warm pool (e.g., Ishii et al., 2004; see also Figs. 1 and 2). A significant portion of the DIC in the upwelled water is either removed by biological uptake or released to the atmosphere during the course of the poleward

and westward advection. Nevertheless, pCO_2sw remains higher than the atmosphere (pCO_2sw–pCO_2air > 90 µatm) due to the effect of concurrent warming (e.g., Feely et al., 1999, 2002, 2006; Ishii et al., 2004; Takahashi et al., 2009a).

The "cold tongue" in the eastern tropics extends to the west during the cold events of ENSO (La Niña) and retreats to the east during the warm events of ENSO (El Niño). ENSO drives changes in the distributions of DIC, SST, and salinity in surface water as well as the surface wind field, and causes large perturbations to pCO_2sw and significant temporal variability in the CO_2 outgassing from the tropical Pacific (e.g., Feely et al., 1987, 2002, 2006; Inoue and Sugimura, 1992; Ishii et al., 2004). The ENSO-driven changes to the variables that control pCO_2sw and the gas transfer coefficient have been simulated and analyzed in a modeling study of Doney et al. (2009a, b). Their analysis revealed that the largest variability in air–sea CO_2 flux in the equatorial Pacific occurs in the region spanning the Date Line to the coast of Peru (Fig. 3). The dominant driver of this variability is the variability in DIC (Fig. 4). Although it is partly offset by the counteracting effect of variability in SST, the effect of DIC-driven changes in pCO_2sw is reinforced by the effect of wind-speed change and results in the large variability in the air–sea CO_2 flux (see Figs. 3 and 4). A number of studies with OBGCMs have examined biogeochemical processes and air–sea CO_2 fluxes over the tropical Pacific (e.g., Winguth et al., 1994, Le Quéré et al., 2000, Obata and Kitamura, 2003, McKinley et al., 2004; Wang et al., 2006; McKinley et al., 2006; Christian et al., 2008; Doney et al., 2009a). These studies have shown the dominant role of the tropical Pacific in the global interannual variability in the oceanic CO_2 uptake.

Underlying the large interannual variability is a secular trend with increasing pCO_2sw observed in this region over the past decades (Feely et al., 1999; Takahashi et al., 2003; Feely et al., 2006). The mean rate of pCO_2sw increase is consistent with the rate of atmospheric CO_2 increase, but decadal modulations have also been reported (Takahashi et al., 2003; Feely et al., 2006; Ishii et al., 2009). The decadal variability of pCO_2sw is possibly linked with changes in the shallow meridional overturning circulation (McPhaden and Zhang, 2002, 2004), but a mechanistic understanding of this connection is still in development.

2.2 North Pacific extratropics

In the extratropics, the dominant timescale of variability is the seasonal cycle. The predominance of this signal is expressed not only in SST, but also in large seasonal variations of mixed layer depth. Such seasonal variations in physical state variables are then associated with important seasonal variability in ocean biogeochemistry and biological activity. The factors drive changes in DIC and pCO_2sw. In the North Pacific, the seasonality of pCO_2sw is particularly significant in the vicinity of the Kuroshio Extension Current and in the western subarctic zone including the western subarctic gyre and the Bering Sea (Takahashi et al., 2002) (Figs. 1 and 2). Throughout the majority of the North Pacific extratropics, particularly in the northern subtropical zone, cooling in winter is the dominant control on low pCO_2sw although it is partly compensated for by increases in DIC associated with wintertime vertical mixing (e.g., Inoue et al., 1987; Takahashi et al., 1993; Ishii et al., 2001; Keeling et al., 2004). By contrast, seasonal variations in pCO_2sw in the western subarctic zone are dominated by the seasonal variations of DIC associated with the enhanced convection in winter and the large net biological DIC consumption in summer (Takahashi et al., 1993, Tsurushima et al., 2002, Chierici et al., 2006).

At interannual to decadal timescales, the dominant mode of basin-scale variability is the Pacific Decadal Oscillation (PDO) (Mantua et al., 1997). Positive PDO anomalies are associated with positive SST anomalies in the Alaskan Gyre and along the west coast of North America, and negative SST anomalies in the central and western North Pacific. While the PDO is expected to impact the distribution of DIC in the upper layers of the North Pacific, the integrated effect of PDO on air–sea CO_2 fluxes remains poorly quantified. Drawing on output from a collection of OBGCMs, McKinley et al. (2006) argued for a correlation of air–sea CO_2 fluxes in the North Pacific with the PDO. Extrapolating from the mechanistic interpretation presented by McKinley et al. (2006), one can posit the following paradigm for the amplitude of interannual variability in the extratropics of the North Pacific, in particular around the subtropical–subarctic frontal zone where the ocean is a strong CO_2 sink in winter: interannual variations in wintertime pCO_2sw are rather small, despite sizable interannual variability in SST, because the opposing effects of SST and DIC concentrations on pCO_2sw compensate each other. This paradigm is consistent with results from the repeated pCO_2sw measurements in the northern subtropics of the western North Pacific at 137° E (Midorikawa et al., 2006). This study demonstrated that the interannual variations in SST and DIC have a counteracting effect on pCO_2sw, and consequently the interannual variability in air–sea CO_2 flux is thought to be associated with the variability in the wind speed. The modeling study of Doney et al. (2009a) came to the same conclusion (Fig. 3). By contrast, larger amplitude interannual variability in pCO_2sw and air–sea CO_2 flux in the subarctic zone and in the eastern subtropics are driven primarily by variability in DIC.

Long-term trends towards increasing pCO_2sw have been observed since the early 1980s along a north–south time-series line to the south of Japan at 137° E (Inoue et al., 1995, Midorikawa et al., 2005, 2012) and at a time-series station near Hawaii (Keeling et al, 2004; Dore et al., 2009). The principal publications to date for basin-scale long-term trends in pCO_2sw are those of Takahashi et al. (2003, 2006) and Lenton et al. (2012), which used existing pCO_2 measurements spanning 1970–2004 and from the mid-1990s to the mid-2000s, respectively. These observations show that the

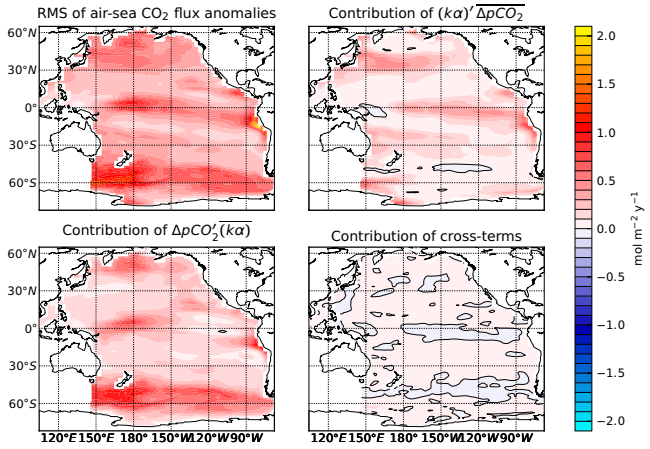

Fig. 3. Partitioning of the mechanisms driving interannual variability in air–sea CO_2 flux (mol m^{-2} yr^{-1}) in the Pacific Ocean in the CCSM ocean BEC model (Doney et al., 2009a). The panels show the root mean square (rms) of the model deseasonalized CO_2 flux anomalies (1990–2009) (top left) and the contributions from gas transfer velocity (wind speed and ice cover) (top right), surface-water ΔpCO_2 (lower left), and the cross-correlation of gas transfer and pCO_2sw anomalies (lower right).

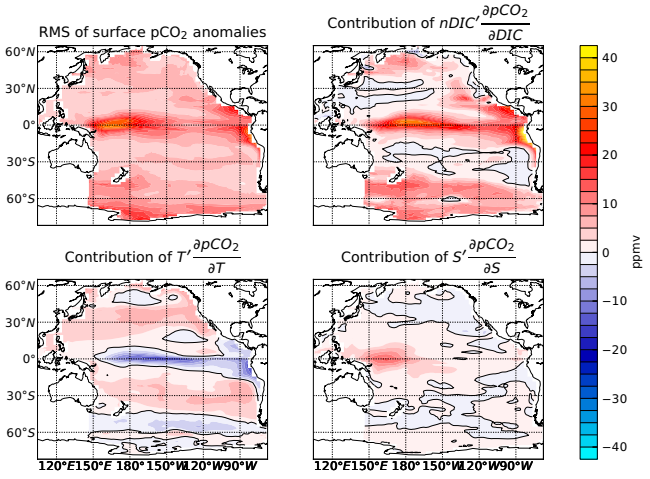

Fig. 4. Partitioning of the mechanisms driving interannual variability in the air–sea pCO_2 difference, ΔpCO_2 (µatm), in the CCSM BEC ocean model. ppmv is numerically equal to ΔpCO_2 (µatm) when the barometric pressure is assumed to be 1.0 atmosphere. The panels show the root mean square of the model deseasonalized surface-water ΔpCO_2 anomalies (1990–2009) (top left) and the contributions from surface-water salinity-normalized dissolved inorganic carbon (top right), temperature (lower left), and fresh water/salinity (lower right). The contributions from salinity-normalized alkalinity (not shown) are generally negligible.

mean rate of pCO_2sw increase is roughly consistent with the rate of atmospheric CO_2 increase, but it is variable both in space and time. Long-term time-series records of oceanic CO_2 appear to show a decrease in the positive trends in pCO_2sw and DIC in the eastern to southern rim of the subtropical cell and in its tropical branch after the strong warm event of ENSO in 1997–1998 (Dore et al., 2003, 2009; Keeling et al., 2004; Ishii et al., 2009; Midorikawa et al., 2012). A change in the subtropical cell (Qiu and Chen, 2010) is a likely driver, but the mechanism driving a decrease in the rate of increasing pCO_2sw and its possible linkage to PDO is not fully understood.

Regarding a potential change in the seasonal cycle in pCO_2sw, Rodgers et al. (2008) and Gorgues et al. (2010) argued that over decadal timescales in the North Pacific there is a divergence between the trend in winter and summer that occurs in the absence of trends in the circulation state of the ocean, and consequently a decadal trend arises towards an increased seasonal cycle. These results found further support in the study of Nakano et al. (2011), who attributed this to the interaction between seasonal dynamics and the changes in carbonate chemistry in seawater with increasing CO_2. This underscores the importance of accounting for the full seasonal cycle when calculating long-term trends, as trends inferred from summer-biased measurements will introduce bias in trend estimates (Lenton et al., 2012).

2.3 South Pacific extratropics

As is the case for the extratropical North Pacific, the extratropical South Pacific is also a major sink for atmospheric CO_2 (Figs. 1 and 2). However, this region poses particular challenges to estimating air–sea CO_2 fluxes due to the paucity of pCO_2sw measurements over this vast sub-basin. The majority of pCO_2sw measurements over the South Pacific have been made in its western region but are less densely distributed than in the North Pacific, and large data gaps in space and time still exist in the eastern South Pacific (Takahashi et al., 2009a). The various gridded data products that have resulted from data synthesis activities of pCO_2sw have by necessity relied on interpolation over large spatial scales and for seasonality in this region.

In the extratropics of the western South Pacific, the dominant timescale of variability in pCO_2sw is likely the seasonal cycle. For the subtropical region of 20–25° S; 165–175° E near Vanuatu, Takahashi et al. (2009a) have shown that the amplitude of seasonal pCO_2sw variations, low in winter and high in summer, is around 40 µatm and the thermodynamic effect of seasonal SST variation is its important controlling factor. However, seasonal pCO_2sw variations have not been well documented for other regions in the extratropics of the South Pacific.

A long-term trend towards increasing pCO_2sw at $+1.30 \pm 0.27$ µatm yr^{-1} from the mid-1980s to mid-2000s has also been reported in the western South Pacific near Vanuatu (Takahashi et al., 2009a). Inoue et al. (1999) have shown an increase of pCO_2sw of $+41 \pm 9$ µatm from January/February 1969 to January/February 1995 for the area 10–45° S, 148–166° E near the east coast of Australia. These

observations show that the mean rate of pCO_2sw increase is roughly consistent with the rate of atmospheric CO_2 increase.

3 Methods

We use a range of air–sea CO_2 flux products in the Pacific Ocean, with these products described below. They are mainly the products collected for the Regional Carbon Cycle Assessment and Processes (RECCAP) (Canadell et al., 2011), but they also include products that have been collected in the preparation of this study for the Pacific Ocean synthesis.

3.1 Climatological pCO_2sw data and pCO_2sw diagnostic models

The evaluation of the air–sea CO_2 flux through gridded pCO_2sw data products was originally developed in the studies built on the database of T. Takahashi for shipboard pCO_2sw measurements (Tans et al., 1990; Takahashi et al., 1997). The database and the gridded data products have been repeatedly updated and widely used since. The analysis here draws upon the data set of gridded monthly climatological pCO_2sw in the reference year 2000 (Takahashi et al., 2009a) (hereafter referred to LDEO V2009; the climatological mean values for $4^\circ \times 5^\circ$ pixel areas are listed in http://www.ldeo.columbia.edu/res/pi/CO2). Diagnostic models of pCO_2sw proposed by Park et al. (2010) and Sugimoto et al. (2012) are also used to estimate seasonal and interannual variations in air–sea CO_2 fluxes. In Park et al. (2010), subannual pCO_2sw-SST relationships have been empirically derived for each $4^\circ \times 5^\circ$ pixel of climatological monthly mean pCO_2sw of LDEO V2009 for the extratropics. For the tropical Pacific, they used empirical pCO_2sw-SST equations that are updated from those of Feely et al. (2006) and are unique for three different time periods of 1979 through 1989, 1990 through mid-1998 and mid-1998 through 2008. Sugimoto et al. (2012) derived the relationships of pCO_2sw versus sea surface salinity, ocean color, year of observation as well as SST for each of 9 sub-regions of the Pacific Ocean from individual pCO_2sw data in Takahashi et al. (2008). These relationships were combined with satellite-derived fields of SST and other parameters to obtain the monthly fields of pCO_2sw. Results from another empirical technique using a neural network (Nakaoka et al., 2013) that has been tested for the Atlantic Ocean (Telszewski et al., 2009) are also included for comparisons in the North Pacific extratropics (Table 1).

A gas transfer velocity (k) is commonly applied to climatological pCO_2sw data and diagnostic models to estimate the air–sea CO_2 flux employing the following functional form (Sweeney et al., 2007; Park et al., 2012):

$$k = 0.25(Sc/660)^{-0.5}\langle U^2\rangle, \quad (1)$$

where Sc is the Schmidt number of CO_2 at SST (Wanninkhof, 1992) and $\langle U^2\rangle$ is monthly mean second moment of wind speed at 10 m height derived from 6-hourly winds at 25 km resolution of the Cross-Calibrated, Multi-Platform (CCMP) Ocean Surface Wind Product (http://podaac.jpl.nasa.gov/DATA_CATALOG/ccmpinfo.html) (Ardizzone et al., 2009; Atlas et al., 2011). The coefficient 0.25 is specific to the wind product used to calculate the air–sea CO_2 flux. It has been optimized globally so that the change in the bomb-^{14}C inventory in the ocean matches atmospheric ^{14}C invasion rate.

Table 1. List of diagnostic models included in this study.

Abbreviation	Reference	Period evaluated[1]
Park_2010	Park et al. (2010)	1990–2009
Sugimoto_2012	Sugimoto et al. (2012)	1990–2009
Nakaoka_2013[2]	Nakaoka et al. (2013)	2002–2008

[1] Period evaluated in this study. For "Park_2010" and "Sugimoto_2012", models have been run for longer.
[2] For the North Pacific extratropics only.

The CO_2 flux (F) is then calculated by the conventional equation for the bulk method:

$$F = k\cdot(C_{sw} - K_0\cdot pCO_2air) = k\cdot K_0\cdot(pCO_2sw - pCO_2air) = k\cdot K_0\cdot\Delta pCO_2, \quad (2)$$

where C_{sw} denotes the concentration of CO_2 in surface seawater and K_0 denotes CO_2 solubility in seawater at a given temperature and salinity. Following the widely used convention for pCO_2 climatologies and diagnostic models, this flux is positive when CO_2 is released from the ocean to the atmosphere and is negative when it is absorbed into the ocean.

3.2 Ocean-interior CO_2 inversion methods

The ocean inversion estimates regional air–sea CO_2 fluxes from ocean-interior observations of DIC and other species from the Global Ocean Data Analysis Project (GLODAP) (Key et al., 2004) and ocean model simulations that describe how fluxes at the surface influence tracer distributions in the interior ocean (e.g. Gloor et al., 2003; Gruber et al., 2009). The inversion initially estimated fluxes from 30 ocean regions, which were subsequently aggregated to 23 regions (10 regions in the Pacific). The anthropogenic and natural air–sea CO_2 fluxes are estimated separately (Mikaloff Fletcher et al., 2006; Mikaloff Fletcher et al., 2007), and the net air–sea fluxes shown here represent a sum of these components and a riverine flux estimate following Jacobson et al. (2007), i.e., $+0.08\,\mathrm{Pg\,C\,yr^{-1}}$ in the North Pacific extratropics and $+0.04\,\mathrm{Pg\,C\,yr^{-1}}$ in the tropical Pacific. These contemporary air–sea CO_2 flux estimates were initially reported in Gruber et al. (2009), but the anthropogenic component has been scaled for this manuscript to match the RECCAP period of 1990–2009. Since this method does not resolve seasonal and

interannual variability, the results are only used to compare the 1990–2009 mean air–sea CO_2 fluxes.

3.3 Ocean biogeochemistry/general circulation models (OBGCMs)

This work also incorporates results from several prognostic ocean biogeochemistry/general circulation model simulations over the period of interest (Table 2). From a total of nine modeling results, seven were retrieved from the RECCAP website (http://www.globalcarbonproject.org/reccap/products.htm). These simulations include not only an account of seasonally and interannually varying air–sea fluxes of CO_2, but also prognostic representations of the processes that are deemed to be important in controlling trends and variations in the ocean carbon cycle. For each case, a prognostic biogeochemistry model is embedded in a physical ocean circulation model and run online. The surface forcing for the dynamical models consists of using atmospheric flux fields derived from a combination of reanalysis and remotely sensed products. Surface buoyancy forcing is accomplished through the use of bulk formulas or other methods for heat and freshwater fluxes, with a restoring of SSS towards climatological values being characteristic of most of the models. The models considered here are coarse resolution models that are neither eddy permitting nor eddy resolving.

Given that the models tend to have differences in their respective (i) underlying physical models, (ii) underlying biogeochemical models, (iii) surface forcing fields, and (iv) handling of river carbon discharge, they should be expected to produce different representations of the ocean carbon cycle. At this point in time, our primary objective will be to provide a description of their similarities and differences. The sensitivity of the modeled carbon cycle to each of these four differences will not be given any extensive consideration in this study. However, we will be providing at least a preliminary assessment of the sensitivity of the differences in the model results, particularly with respect to the sensitivity of the carbon cycle to physical forcing at the sea surface in Sect. 6.1.

3.4 Ocean pCO_2sw data assimilation

The pCO_2sw data set of LDEO V2009 has also been assimilated into an offline tracer transport model (OTTM; Valsala and Maksyutov, 2010). This assimilation system minimizes the model biases in the surface ocean pCO_2 through a weak constraint given to its gridded monthly climatology of LDEO V2009, while a strong constraint is given to the in situ ship-observed pCO_2sw measurements whenever they are available in the LDEO database (Takahashi et al. 2009b). The weak constraint is further weighted by the inverse of the model interannual variance, which ensures that the model is constrained to the monthly climatological pCO_2sw only in regions where the interannual variability is small. Assimilated data of pCO_2sw and air–sea CO_2 flux were constructed from 1996–2008 using this method, while here we present an extended record of the data starting from 1990. Prior to 1996, the data represent the model interannual variability summed to the monthly climatology derived from the assimilation period of 1996–2008.

3.5 Atmospheric CO_2 inversion methods

An atmospheric CO_2 inversion intercomparison project community was launched by the TransCom with the RECCAP initiative collecting a number of atmospheric CO_2 inversion results and comparing those to synthesize general features of the recent state-of-the-art inversions. The results are archived at the web site https://transcom.lsce.ipsl.fr/ representing 14 different approaches. Peylin et al. (2013) selected 11 inversion results from those and presented long-term mean, long-term trend, interannual variations and mean seasonal variations separately for land and ocean regions in the tropics and northern and southern extratropics.

The analysis here includes the inversion results for the Pacific Ocean region from the total of six atmospheric CO_2 inversions with outputs longer than 17 yr for decadal mean flux and ten models for mean seasonal variations (Table 3). It should be noted here that they differ in the atmospheric CO_2 data sets (i.e., observational constraints), atmospheric transport models, spatial resolution of the optimized flux and inversion methods. Most of the inversions used climatological air–sea CO_2 flux data from some versions of the LDEO monthly climatology as a prior air–sea CO_2 flux estimate, and therefore regionally integrated or seasonal variations of posterior net air–sea CO_2 fluxes have been constrained by it to a greater or lesser extent depending on the inversion method.

4 Regions of assessment

We provide regionally integrated net air–sea CO_2 fluxes over three sub-basins of the Pacific Ocean that are zonally partitioned. They are the zone to the north of 18° N including the Bering Sea ($< 66°$ N), the tropical zone bounded by 18° N and 18° S, and the southern zone bounded by 18 and 44.5° S (Fig. 5). The region to the south of 44.5° S is discussed in Lenton et al. (2013). The boundaries separating these three sub-basins are chosen to be consistent with previous publications, grouping 10 prescribed ocean regions of the ocean CO_2 inversions in the Pacific (Mikaloff Fletcher et al., 2006, 2007; Gruber et al., 2009). As such, these divisions are fairly consistent with dynamical boundaries separating the subtropical gyres of the North Pacific and the South Pacific from the Tropical Pacific.

The tropical zone defined here (18° N–18° S) includes a small part of the equatorward flanks of the subtropical gyres of the North and South Pacific. Nevertheless, the tropical zone mainly consists of the "warm pool" in the west and

Table 2. List of prognostic ocean biogeochemistry/general circulation models and a pCO_2sw data-assimilation system included in this study.

Name	Abbreviation	Reference	Period evaluated[1]
CCSM-BEC	BEC	Doney et al. (2009a, b)	1990–2009
MICOM-HAMOCCv1	BER	Assmann et al. (2010)	1990–2009
CSIRO-BOGCM	CSIRO	Matear and Lenton (2008)	1990–2009
CCSM-ETHk15[2]	ETHk15	Graven et al. (2012)	1990–2007
MOM4-TOPAZ	GFDL	Dunne et al. (2012)	1990–2004
NEMO-PISCES[3]	IPSL	Aumont and Bopp (2006)	1990–2009
MRI.COM	MRI	Nakano et al. (2011)	1990–2007
NEMO-PlankTOM5NCEP[3,4]	UEA_CEP1	Buitenhuis et al. (2010)	1990–2009
NEMO-PlankTOM5CCMP[3,5]	UEA_CCMP	Buitenhuis et al. (2010)	1990–2009
OTTM-CO2 assimilation	OTTM	Valsala and Maksyutov (2010)	1990–2008

[1] Period evaluated in this study. Models have been run for longer.
[2] ETHk15: CCSM-ETH model with a prescribed global average gas transfer velocity of 15 cm h^{-1}.
[3] River carbon discharge has been considered.
[4] UEA_NCEP: NEMO-PlankTOM5 model with NCEP core forcing.
[5] UEA_CCMP: NEMO-PlankTOM5 model with NCEP core forcing (heat, precipitation etc.) but using CCMP winds for both ocean circulation and gas exchange.

Table 3. List of atmospheric CO_2 inversions included in this study.

Abbreviation	References	Period evaluated*
LSCE an v2.1	Piao et al. (2004)	1996–2004
LSCE var v1.0	Chevallier et al. (2010)	1990–2008
C13 CCAM law	Rayner et al. (2008)	1992–2008
C13 MATCH rayner	Rayner et al. (2008)	1992–2008
CTracker US	Peters et al. (2007)	2001–2008
JENA s96 v3.3	Rödenbeck (2005)	1996–2008
RIGC patra	Patra et al. (2005)	1993–2006
JMA 2010	Maki et al. (2010)	1990–2008
TRCOM mean 9008	Baker et al. (2006)	1990–2008
NICAM niwa	Niwa et al. (2012)	1990–2007

* Period evaluated in this study. Some inversions may have been run for longer time.

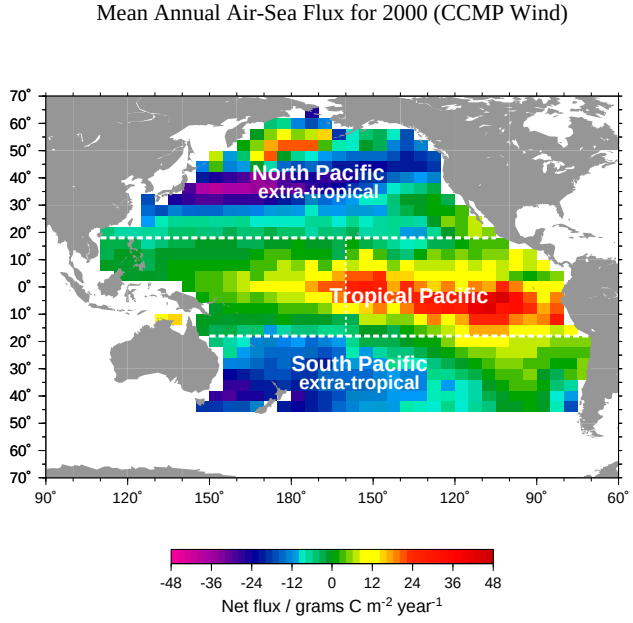

Fig. 5. Three Pacific Ocean sub-basins defined according to the aggregation of 14 Pacific regions of the ocean-interior CO_2 inversions (Mikaloff Fletcher, 2006). Superposed is the mean annual air–sea CO_2 flux for the year 2000 calculated with climatological pCO_2sw of LDEO V2009 (Takahashi et al., 2009a) and CCMP wind (Ardizzone et al., 2009; Atlas et al., 2011). Positive fluxes are out of ocean and negative fluxes are into the ocean.

the "cold tongue" in the east. The "cold tongue" includes both the equatorial and the Peruvian divergence systems. In Sect. 5.1, the interannual variability in the western tropical zone to the west of 160° W and the eastern tropical zone to the east of 160° W are presented separately in order to see the effect of westward expansions of the "cold tongue" during the ENSO cold events.

The North Pacific to the north of 18° N encompasses most of the subtropical gyre and the entire subarctic zone. As shown in Figs. 1 and 2, seasonality of pCO_2sw reverses within this domain. In winter, pCO_2sw decreases to considerable CO_2 undersaturation with respect to atmospheric CO_2 in the northern subtropics due to the large effect of seasonal cooling, and pCO_2sw increases to the point of supersaturation in the subarctic region due to the large effect of DIC increase associated with vertical convection. In contrast, during the summer, pCO_2sw increases to being in near equilibrium with respect to the atmosphere in the subtropics due to seasonal warming, and pCO_2sw decreases in the subarctic region due to the DIC decrease associated with biological production. The air–sea CO_2 flux shown for the North Pacific extratropics is the integrated flux over these two subdomains.

The extratropical zone between 18 and 44.5° S covers most of the subtropical gyre in the South Pacific. We note that the southern boundary at 44.5° S lies in the vicinity of the Subtropical Convergence Zone and the surface water in this zone is the large sink of the atmospheric CO_2 (Metzl et al., 1999; Inoue et al., 1999; Takahashi et al., 2009a). Therefore, the estimate of air–sea CO_2 flux in the South Pacific extratropics is expected to depend largely on the choice of the southern boundary. We will examine this using LDEO V2009 climatological fluxes in Sect. 5.3.

For each sub-basin, regionally integrated air–sea CO_2 fluxes were calculated as monthly means from each product: monthly climatological pCO_2sw data of LDEO V2009, pCO_2sw diagnostic models, Ocean BGC models, a pCO_2sw data assimilation, and atmospheric CO_2 inversions. Decadal and longer-term mean fluxes were then calculated over the intervals 1990–1999 and 2000–2009, as well as over the combined period 1990–2009. They were subsequently compiled for each of the approaches: the average ± range for pCO_2sw diagnostic models and the median ± median absolute deviation (MAD) for OBGCMs and atmospheric CO_2 inversions were calculated for decadal and longer-term means. In addition, skill-weighted mean values have been given for ocean CO_2 inversions. However, no remarkable differences are seen in decadal mean flux between 1990–1999 and 2000–2009 in all approaches (Fig. A1). Therefore, in the following sections, we will not mention the decadal means but present only longer-term means for the period 1990–2009 and interannual variability and mean seasonal variability for this period. For the pCO_2sw data assimilation and the atmospheric CO_2 inversions, mean fluxes were calculated for 1990–2008 since modeling products in the year 2009 were not available. In the cases of pCO_2sw diagnostic models and OBGCMs, differences in the mean fluxes between for 1990–2009 and for 1990–2008 were minimal ($< 0.01\,\mathrm{Pg\,C\,yr^{-1}}$). Therefore we assume that the comparison of mean and median fluxes for 1990–2009 of diagnostic models and OBGCMs and those for 1990–2008 of pCO_2sw data assimilation and atmospheric CO_2 inversions are not problematic in the following discussions.

5 Results

5.1 Tropical Pacific 18° S–18° N

From the LDEO V2009 climatological pCO_2sw data set (which has been filtered to remove the ENSO warm events) and CCMP monthly wind speed, the annual CO_2 flux from the tropical Pacific is estimated to be $+0.51 \pm 0.24\,\mathrm{Pg\,C\,yr^{-1}}$ in year 2000 (Table 4; Fig. 6), which comprises a small efflux ($+0.06\,\mathrm{Pg\,C\,yr^{-1}}$) from the western tropical sector (west of 160° W), and a larger efflux ($+0.45\,\mathrm{Pg\,C\,yr^{-1}}$) from the eastern tropical sector. The mean of the time-averaged air–sea CO_2 flux from the two diagnostic models (which include the ENSO warm events) considered here ($+0.52 \pm 0.09\,\mathrm{Pg\,C\,yr^{-1}}$) is consistent with the estimates from the climatological pCO_2sw and the atmospheric CO_2 inversions ($+0.53 \pm 0.08\,\mathrm{Pg\,C\,yr^{-1}}$). These diagnostic models also showed a peak-to-peak amplitude of interannual variability of $0.27 \pm 0.07\,\mathrm{Pg\,C\,yr^{-1}}$ between 1990 and 2009 (Table 4; Fig. 7). Negative anomalies of air–sea CO_2 flux are associated with the ENSO warm events. The negative anomaly is particularly significant in the eastern tropical sector during the ENSO strong warm event that occurred in 1997–1998 when the negative anomaly of the flux reached a level of -0.29 and $-0.14\,\mathrm{Pg\,C\,yr^{-1}}$, depending on the diagnostic model. This strong warm event was immediately followed by the persistent ENSO cold event in 1998–2000 with quite large positive anomalies in the western sector (up to +0.11 and $+0.17\,\mathrm{Pg\,C\,yr^{-1}}$) as well as in the eastern sector (+0.08 and $+0.09\,\mathrm{Pg\,C\,yr^{-1}}$) (Fig. 7). The results of pCO_2sw data assimilation also shows the interannual variability of air–sea CO_2 flux that is associated with the ENSO, although the negative anomaly during the 1997–1998 warm event was smaller ($-0.14\,\mathrm{Pg\,C\,yr^{-1}}$).

The median ± MAD of time-averaged air–sea CO_2 flux in the tropical Pacific evaluated by OBGCMs is $+0.39 \pm 0.04\,\mathrm{Pg\,C\,yr^{-1}}$ for 1990–2009. This is in good agreement with the estimate from ocean-interior CO_2 inversion methods ($+0.37 \pm 0.12\,\mathrm{Pg\,C\,yr^{-1}}$), but is $0.13\,\mathrm{Pg\,C\,yr^{-1}}$ smaller than the estimate from the two diagnostic models considered here. Given the considerable range of flux estimates in both diagnostic models (+0.44 to $+0.61\,\mathrm{Pg\,C\,yr^{-1}}$) and the OBGCMs (+0.25 to $+0.55\,\mathrm{Pg\,C\,yr^{-1}}$), it is important to compare the pCO_2sw fields and gas exchange coefficients to provide more clarity about these differences. One of the potential sources of the differences is the choice of wind-speed product used to force the ocean circulation in OBGCMs as well as to compute the CO_2 gas transfer velocities that are used both in diagnostic models and OBGCMs. Park et al. (2010) have shown that the global mean air–sea CO_2 flux changes by as much as 20 % with the choice of wind-speed products and coefficient for gas transfer velocity for gas exchange in their diagnostic model. We will discuss this in more detail in Sect. 6.1 for a diagnostic model and for an OBGCM.

In terms of the phase of interannual variability, the results from most OBGCMs are consistent with those from diagnostic models demonstrating larger CO_2 efflux during the ENSO cold events and smaller efflux during the warm events. However, OBGCMs appear more sensitive to the ENSO warm and cold events (Table 4 and Fig. 7), particularly during the 1995–1996 cold event and during the 1997–1998 warm event. The reason for the larger ENSO sensitivity in OBGCMs than diagnostic models is yet to be determined but is likely to be attributable to the larger response of the pCO_2sw field to the change in the wind field (see Sect. 6.1) associated with the ENSO events. It is also likely that diagnostic models more or less smooth out the variability through

Table 4. Mean and amplitude of interannual variability (IAV) of regionally integrated air–sea CO_2 flux in the sub-basins of the Pacific Ocean for the period 1990–2009. All units are Pg C yr^{-1}.

Regions [Area (km^2)]		LDEO V2009[1]	pCO_2sw Diag. Models[2]	Ocean Inv.[3]	OBGC Models[4]	OBGCM +Riverine flux[5]	pCO_2sw Data Assim.[6]	Atm. Inv.[4,6]	Best Estimates[7]
North Pacific extratropics	Mean	−0.44 ±0.21	−0.52 ±0.05 ±0.25	−0.42 ±0.08	−0.57 ±0.02	−0.49 ±0.02	−0.37	−0.48 ±0.08	−0.47 ±0.13
66–18° N [4.43×10^7]	IAV[8]		0.12 ±0.02		0.11 ±0.02		0.19	0.41 ±0.06	
Tropical Pacific	Mean	+0.51 ±0.24	+0.52 ±0.09 ±0.25	+0.37 ±0.12	+0.39 ±0.04	+0.41 ±0.05	+0.27	+0.53 ±0.08	+0.44 ±0.14
18° N–18° S [6.65×10^7]	IAV[8]		0.27 ±0.07		0.40 ±0.09		0.34	0.48 ±0.15	
South Pacific extratropics	Mean	−0.29 ±0.14	−0.28 ±0.00 ±0.13	−0.46 ±0.10	−0.39 ±0.11	−0.39 ±0.11	−0.24	−0.29 ±0.08	−0.37 ±0.08
18–44.5° S [3.88×10^7]	IAV[8]		0.08 ±0.03		0.12 ±0.03		0.11	0.64 ±0.11	
All Pacific	Mean	−0.22 ±0.35	−0.27 ±0.13 ±0.38	−0.52 ±0.18	−0.57 ±0.12	−0.45 ±0.18	−0.33	−0.26 ±0.10	−0.40 ±0.21
66° N–44.5° S [14.96×10^7]	IAV[8]		0.25 ±0.20		0.49 ±0.08		0.45	1.08 ±0.29	

[1] Climatological flux at year 2000 calculated with CCMP wind product. Error of ±48 % are applied to the flux in each sub-basin and error of ±sqrt {$\sum$ (error in a sub-basin)^2} is applied for the all Pacific. Components of error assumed is ±10 % for ΔpCO_2, ±30 % for gas transfer scaling factor (0.25), ±20 % for wind speed, ±25 % for normalization for the year 2000, ±15 % for under sampling (based on SST).
[2] Mean ± half of range of two diagnostic models of Park et al. (2010) and Sugimoto et al. (2012) and ±48 % error as in the LDEO V2009 climatological fluxes.
[3] Skill-weighted average ± standard deviation of the ocean CO_2 inversions.
[4] Median ± median absolute deviation of estimates from various models and inversions.
[5] No errors in the riverine CO_2 flux is considered.
[6] For the period 1990–2008.
[7] The estimates given here are the mean values from the pCO_2sw diagnostic models and ocean inversions. Uncertainty has been given as sqrt {$(0.5)^2 \cdot$ sigma(Diag)$^2 + (0.5)^2 \cdot$ sigma(OcnInv)^2}.
[8] Interannual variability, i.e., peak-to-peak difference of the annual mean flux.

the regression analyses of pCO_2sw as a function of SST and other parameters that are used to correct the implicated undersampling in observations. To date, two modeling studies have evaluated the skill of the diagnostic method originally developed by Lee et al. (1998) and Loukos et al. (2000) in simulating air–sea CO_2 flux variability over the tropical Pacific (Christian et al., 2008; Park et al., 2010). For both studies, outputs of three-dimensional (x, y, t) fields of SST and other parameters in the tropical ocean are sampled from an OBGCM, and three-dimensional field of pCO_2sw is reconstructed with a diagnostic model. The air–sea CO_2 flux is then calculated from the reconstructed pCO_2sw field using the same gas exchange coefficient as in the OBGCMs, and this estimate is compared with the fully resolved explicit fluxes in the model. The study of Christian et al. (2008) argued that diagnostic models can underestimate the amplitude of interannual variability in the flux from tropical Pacific by up to a factor of 50 % depending on the model and grid resolution used. The study of Park et al. (2010) also found that their diagnostic model underestimates 15–20 % of the variability, while it overestimates 25–30 % for the full fluxes, in the tropical Pacific. The estimates of air–sea CO_2 flux in the tropical Pacific from the atmospheric CO_2 inversions used in this study showed large monthly fluctuations that are not seen in the estimates from diagnostic models and OBGCMs (Fig. 7). Inverse estimates for tropical regions are subject to a high degree of uncertainty due to the limited number of observing stations in this region. Nevertheless, many of the atmospheric CO_2 inverse models show a decrease in outgassing during the strong ENSO warm event in 1997–1998 and an increase during the persistent cold event over 1998–2000.

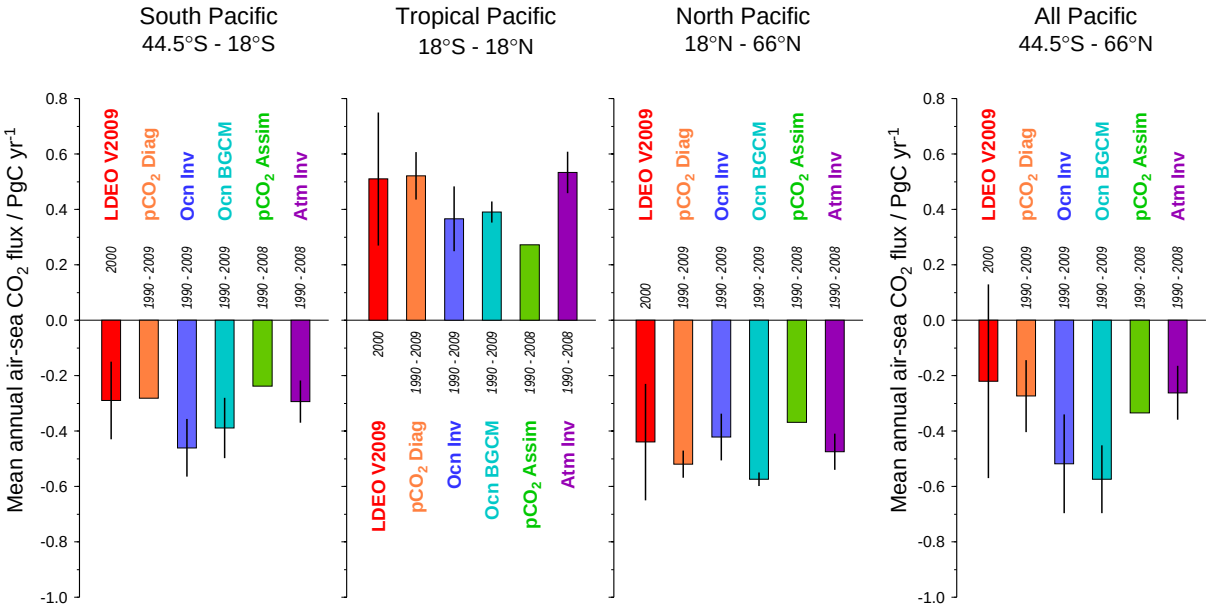

Fig. 6. Summary of regionally integrated and time-averaged net air–sea CO_2 flux (Pg C yr^{-1}) in the Pacific Ocean sub-basins shown in Fig. 5.

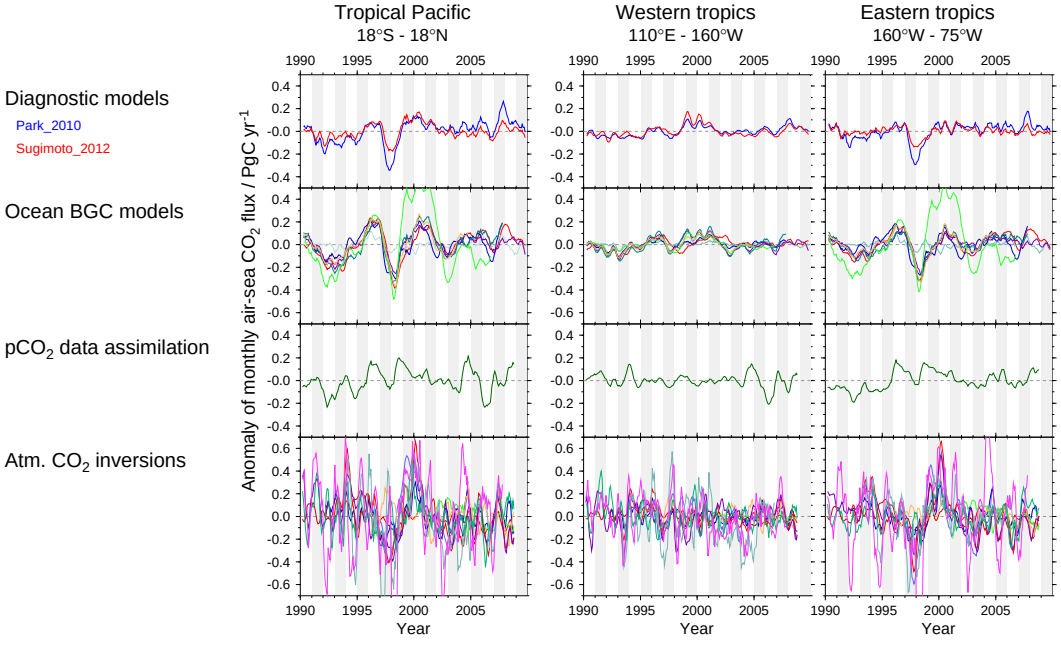

Fig. 7. Trend of air–sea CO_2 flux anomalies (5-month running means) in the tropical Pacific (18° S–18° N) (left panel) for 1990–2009, and its components in the western tropical sector to the west of 160° W (middle) and in the eastern tropical sector to the east of 160° W.

5.2 North Pacific extratropics 18–66° N

The mean annual air–sea CO_2 flux in the North Pacific extratropics north of 18° N is estimated to be -0.44 ± 0.21 Pg C yr^{-1} in year 2000 from the LDEO V2009 climatological pCO_2sw fields, and -0.47 and -0.57 Pg C yr^{-1} for the period 1990–2009 from diagnostic models of Park et al. (2010) and Sugimoto et al. (2012), respectively. An independent diagnostic model of Nakaoka et al. (2013) that uses a non-linear empirical neural network technique also suggests similar, but slightly smaller, mean influx (-0.40 Pg C yr^{-1}) into this domain for the period 2002–2008. This is 0.07 and 0.20 Pg C yr^{-1} smaller, respectively, than the CO_2 flux estimates from the two other diagnostic models for the same period (-0.47 and -0.60 Pg C yr^{-1}). Since the same wind product has been

used to calculate the gas exchange coefficient, these differences in the flux estimate are attributable to the differences in the pCO_2sw field. The strong CO_2 uptake in the North Pacific is dominated by the uptake in the northern subtropics and subtropical-to-subarctic transition zone in winter (Fig. 1), where the effect of cooling on pCO_2sw is stronger than the effect of DIC increase due to vertical mixing (Ishii et al., 2001; Takahashi et al., 2002). The mean annual air–sea CO_2 flux in the same sub-basin from pCO_2sw data assimilation ($-0.37\,\mathrm{Pg\,C\,yr^{-1}}$) is somewhat smaller, but those from ocean-interior CO_2 inversions ($-0.42 \pm 0.08\,\mathrm{Pg\,C\,yr^{-1}}$) and atmospheric CO_2 inversions ($-0.48 \pm 0.08\,\mathrm{Pg\,C\,yr^{-1}}$) are consistent with the range of estimates from LDEO V2009 climatological pCO_2sw fields and diagnostic models. The net CO_2 sink estimated by the OBGCMs ($-0.57 \pm 0.02\,\mathrm{Pg\,C\,yr^{-1}}$) is the strongest among the estimates from the various approaches.

The peak-to-peak difference of the interannual variability in the air–sea CO_2 fluxes derived from diagnostic models over the North Pacific extratropics is small ($0.12\,\mathrm{Pg\,C\,yr^{-1}}$) (Fig. 8 and Table 4). This is also the case for the OBGCMs. Most of these models show slightly positive anomalies ($\sim 0.1\,\mathrm{Pg\,C\,yr^{-1}}$) for the period of 1999–2001 when the PDO index tended to be negative, but the relationship between the anomaly of CO_2 flux and the PDO is not discernible for other periods. The amplitude of interannual variability is somewhat larger in the flux estimate from pCO_2sw data assimilation ($0.19\,\mathrm{Pg\,C\,yr^{-1}}$). Valsala et al. (2012) posited a "four-region" structure in the North Pacific air–sea CO_2 flux variability related to the PDO in the data assimilation product. However, the correlation of the air–sea CO_2 flux with PDO is not clear when averaged over the North Pacific extratropics. Most of the atmospheric CO_2 inversions show negative anomalies around the late 1994, 1997, 2001 and early 2007 and positive anomalies around early 1994 and 2004. However, the correlations with the PDO index are also not obvious. No consistent pattern of interannual variability of air–sea CO_2 flux is seen among the different approaches in the North Pacific extratropics, suggesting that the various methods have not yet converged in their representation of interannual-to-decadal variability over the North Pacific extratropics.

With regard to the seasonality of air–sea CO_2 flux in the North Pacific extratropics, results from the three diagnostic models are consistent in that they all show very small net air–sea CO_2 flux in summer (July–September: $+0.03 \pm 0.10\,\mathrm{Pg\,C\,yr^{-1}}$) and a larger influx into the ocean in winter (January–March: $-0.86 \pm 0.20\,\mathrm{Pg\,C\,yr^{-1}}$) (Fig. 9). The difference in the net annual air–sea CO_2 flux among these diagnostic models is mainly attributable to the difference in the flux estimates in the cold time of year (December–April). The phase of seasonality in the pCO_2sw data assimilation product is consistent with diagnostic models but does show a net CO_2 efflux in summer ($+0.56\,\mathrm{Pg\,C\,yr^{-1}}$ in July). All OBGCMs presented in this work also show well-defined seasonality with large CO_2 sink in winter (-1.86 to $-1.04\,\mathrm{Pg\,C\,yr^{-1}}$) and slightly negative or moderately positive flux in summer (-0.03 to $+0.64\,\mathrm{Pg\,C\,yr^{-1}}$). By contrast, in the atmospheric CO_2 inversions large sub-annual variations are found in the air–sea CO_2 flux but its seasonality remains poorly resolved.

5.3 South Pacific extratropics 44.5–18° S

The climatological net annual air–sea CO_2 flux for the year 2000 evaluated from LDEO V2009 climatological pCO_2sw was $-0.29 \pm 0.14\,\mathrm{Pg\,C\,yr^{-1}}$, and the long-term mean net annual air–sea CO_2 flux over two decades after 1990 was $-0.28 \pm 0.00\,\mathrm{Pg\,C\,yr^{-1}}$ from the diagnostic models and $-0.29 \pm 0.08\,\mathrm{Pg\,C\,yr^{-1}}$ from the atmospheric CO_2 inversions, respectively. The strength of the CO_2 sink in the South Pacific extratropics is smaller than that in the North Pacific extratropics (-0.44 to $-0.52\,\mathrm{Pg\,C\,yr^{-1}}$) estimated by the same approaches. The smaller sink in the South Pacific extratropics is, in part, ascribed to its smaller area defined here (18–44.5° S; $3.88 \times 10^7\,\mathrm{km^2}$) than in the North Pacific extratropics (18–66° N; $4.43 \times 10^7\,\mathrm{km^2}$), but it is primarily attributable to the difference in the zonal distributions of air–sea CO_2 flux. In the North Pacific extratropics, there is a band serving as a strong CO_2 sink that extends over the mid-latitudes from the region off of Japan to off of the west coast of North America (Figs. 1 and 5). The CO_2 sink is particularly strong around the subtropical-to-subarctic transition zone where the net annual air–sea CO_2 flux from climatological pCO_2sw of LDEO V2009 reaches $-2.9\,\mathrm{mol\,m^{-2}\,yr^{-1}}$. The western South Pacific extratropics near Australia and New Zealand is also a region of CO_2 sink but its strength is moderate (ca. $-2.1\,\mathrm{mol\,m^{-2}\,yr^{-1}}$). In addition, the eastern South Pacific extratropics is a weak sink or even a weak source of CO_2 to the atmosphere. However, it has to be noted that the South Pacific extratropics is severely undersampled for pCO_2sw in winter (Takahashi et al., 2009a) and the uncertainty in the air–sea CO_2 flux is thereby considerably larger there than it is over the North Pacific. The integrated flux over this region is also sensitive to the choice of the southern boundary of the South Pacific extratropics. In this analysis, the South Pacific extratropics have been defined to be the region north of 44.5 to 18° S. According to the LDEO V2009 climatological pCO_2sw, the net annual CO_2 flux integrated over the zonal band between 42 and 46° S in the South Pacific is $-0.056\,\mathrm{Pg\,C\,yr^{-1}}$. This accounts for ca. 20 % of net CO_2 sink in the South Pacific extratropics.

The results from OBGCMs for the South Pacific extratropics show a large range of estimates (-0.19 to $-0.71\,\mathrm{Pg\,C\,yr^{-1}}$) for the net air–sea CO_2 flux averaged over the period 1990–2009. In addition, their median ($-0.39 \pm 0.11\,\mathrm{Pg\,C\,yr^{-1}}$) indicate a $0.1\,\mathrm{Pg\,C\,yr^{-1}}$ larger sink than the estimates from other methods that are constrained by the data of pCO_2sw. The larger range of air–sea CO_2 fluxes here presents a marked contrast to the rather small

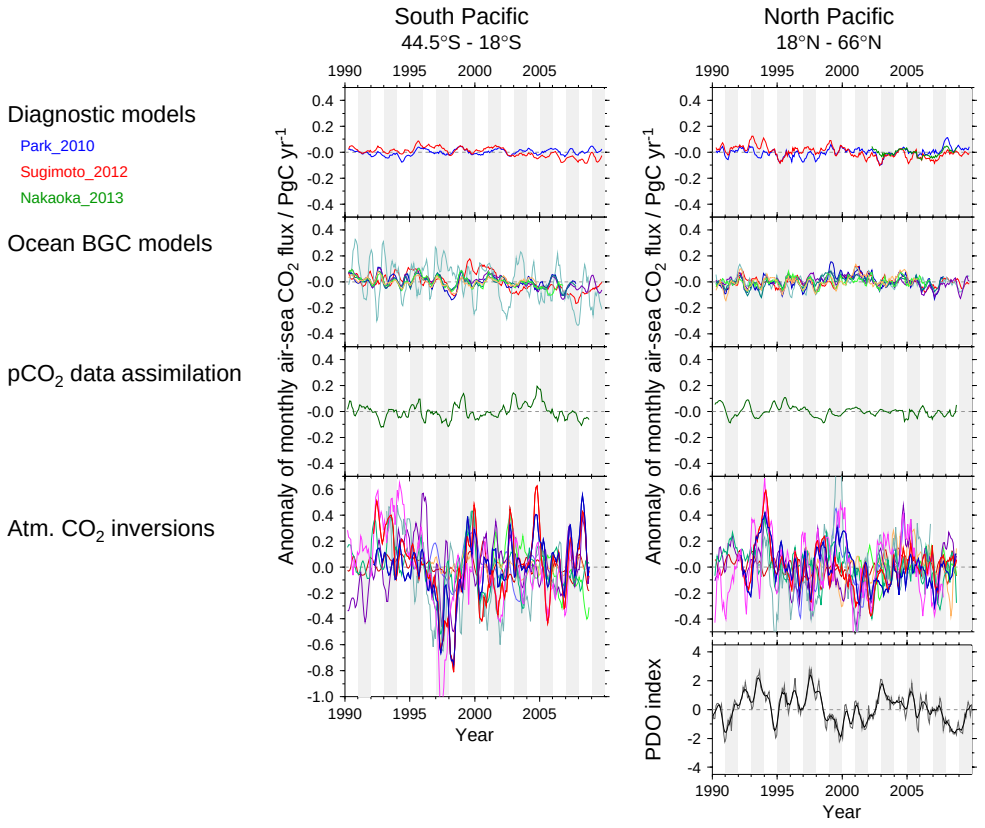

Fig. 8. Trend of air–sea CO_2 flux anomalies (5-month running means) in the South Pacific extratropics (44.5–18° S) (left) and in the North Pacific extratropics (18–66° N) (right) for 1990–2009. Also shown at the bottom of right panel is the Index of Pacific Decadal Oscillation (http://ds.data.jma.go.jp/tcc/tcc/products/elnino/decadal/pdo.html).

range of OBGCM estimates in the North Pacific extratropics (-0.57 ± 0.02 Pg C yr^{-1}). In the South Pacific extratropics, the estimates of air–sea CO_2 flux by OBGCMs are split into two groups. For the two models that show a larger CO_2 sink, the averaged (±standard deviation) flux is -0.71 ± 0.02 Pg C yr^{-1}, while for the remaining six models a smaller CO_2 sink of -0.32 ± 0.08 Pg C yr^{-1} is seen, which is more consistent with LDEO V2009 climatology and diagnostic models.

The weighted average of net air–sea CO_2 flux from the ocean CO_2 inversions is -0.46 ± 0.10 Pg C yr^{-1}. This shows nearly a 0.2 Pg C yr^{-1} larger sink than the estimates from climatological pCO_2sw and diagnostic models. Only the results from ocean-interior CO_2 inversions show a larger oceanic CO_2 sink in the South Pacific extratropics than in the North Pacific extratropics.

With regard to the interannual variations, no remarkable change is seen in the diagnostic models (Fig. 8 and Table 4). The estimate from Sugimoto et al. (2012) shows small positive anomalies for 1995–1997 and small negative anomalies for 2006–2008, but they are within ± 0.1 Pg C yr^{-1}. Two of the OBGCMs show a larger CO_2 sink in the South Pacific extratropics and also show larger interannual variation with the amplitude of ± 0.23 and ± 0.38 Pg C yr^{-1}, but the variations are smaller (< 0.13 Pg C yr^{-1}) in the other six OBGCMs that show smaller net CO_2 sinks. The latter six OBGCMs consistently show negative anomalies averaging about -0.1 Pg C yr^{-1} in 1998. However, no such anomaly is seen in 1998 in the diagnostic models. In general, the atmospheric CO_2 inversions again show much larger interannual variations than the other approaches. This is likely to be attributed to the few data covering land regions in the Southern Hemisphere, such that the atmospheric CO_2 inversions are not able to effectively distinguish between air-land CO_2 flux and air–sea CO_2 flux. Most of the results from the atmospheric CO_2 inversions show large negative anomalies in 1997–1998 (-0.23 Pg C yr^{-1} on the average) that are larger than the anomalies found in the OBGCMs.

With regard to the seasonality of air–sea CO_2 fluxes over the South Pacific extratropics, results from the LDEO V2009 climatological pCO_2sw and two diagnostic models agreed within ± 0.04 Pg C yr^{-1} in all months. As in the North Pacific extratropics, they all show a very small net air–sea CO_2 flux in summer (February: -0.00 ± 0.02 Pg C yr^{-1}) and a larger influx into the ocean in winter (August: -0.56 ± 0.01 Pg C yr^{-1}). However, the

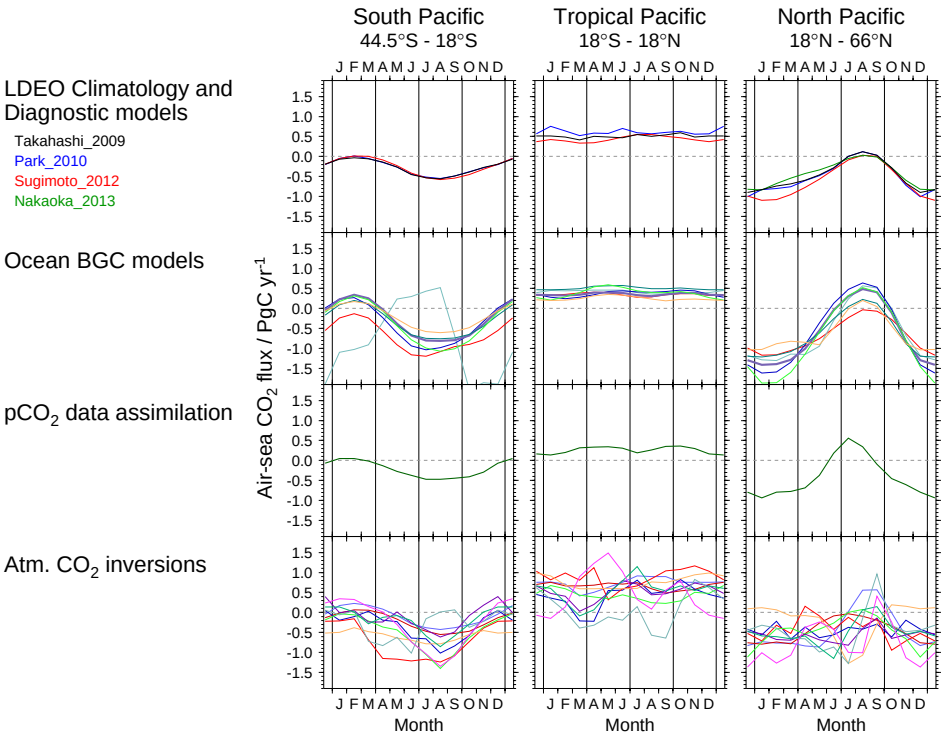

Fig. 9. Mean monthly variations of air–sea CO_2 flux in the South Pacific extratropics (44.5–18° S) (left), in the tropical Pacific (18° S–18° N) (middle) and in the North Pacific extratropics (18–66° N) (right) for 1990–2009.

amplitude of seasonal cycle in the South Pacific extratropics is about 2/3 of that in the North Pacific extratropics (Fig. 9). The phase and amplitude of seasonality in the flux from the pCO_2sw data assimilation product is also consistent with LDEO V2009 and diagnostic models. Most OBGCMs presented in this work also show well-defined seasonality with a large CO_2 sink in winter (-1.20 to $-0.60\,\mathrm{Pg\,C\,yr^{-1}}$) and slightly negative or moderately positive fluxes in summer (-0.13 to $+0.50\,\mathrm{Pg\,C\,yr^{-1}}$). The median ± MAD of the amplitude of seasonality is $1.15 \pm 0.18\,\mathrm{Pg\,C\,yr^{-1}}$, which is again about 2/3 of that in the North Pacific extratropics ($1.88 \pm 0.40\,\mathrm{Pg\,C\,yr^{-1}}$). Most atmospheric CO_2 inversions also resolved the seasonality of the air–sea CO_2 fluxes in the South Pacific extratropics with a larger ocean CO_2 sink in winter and a smaller net flux in summer. The median ± MAD of the amplitude of seasonality is $1.01 \pm 0.36\,\mathrm{Pg\,C\,yr^{-1}}$. This is about twice as large as that from the LDEO V2009 climatological pCO_2sw and the two diagnostic models, but it agrees well with the results from the OBGCMs.

5.4 All Pacific Ocean regions 44.5° S–66° N

The time-averaged air–sea CO_2 flux for 1990–2009 described in the previous sections reveals a quite large range of variation among the different approaches when integrated over the Pacific Ocean between 44.5° S and 66°N (Table 4 and Fig. 6). It ranges from the weak CO_2 sink of $-0.22\,\mathrm{Pg\,C\,yr^{-1}}$ that was estimated from LDEO V2009 climatological pCO_2sw to a stronger sink of $-0.57 \pm 0.12\,\mathrm{Pg\,C\,yr^{-1}}$ from OBGCMs. The results from diagnostic models ($-0.27 \pm 0.13\,\mathrm{Pg\,C\,yr^{-1}}$), pCO_2sw data assimilation ($-0.33\,\mathrm{Pg\,C\,yr^{-1}}$) and atmospheric CO_2 inversions ($-0.26 \pm 0.10\,\mathrm{Pg\,C\,yr^{-1}}$) that are more or less constrained by the measurements of pCO_2sw are consistent with the estimate from the climatological pCO_2sw. However, the estimate from the ocean-interior CO_2 inversions ($-0.52 \pm 0.18\,\mathrm{Pg\,C\,yr^{-1}}$) is similar to the results from the OBGCMs. The smaller efflux from the tropics and larger or comparable influxes into the extratropics cooperatively contribute to the estimate of larger CO_2 influx into the Pacific from the OBGCMs and ocean-interior CO_2 inversions. It is also interesting to note that the efflux from the tropics tends to be balanced by the influx into the North Pacific extratropics in the diagnostic models, but it tends to be balanced with the influx into the South Pacific extratropics in the estimate from the OBGCMs.

In regard to the interannual variability, the diagnostic models and OBGCMs are consistent with each other in that the ENSO-driven change in the tropical zone is playing a dominant role in the Pacific, and changes in the extratropics are minor as mentioned in Sects. 5.2 and 5.3 (Fig. 10). In the pCO_2sw data assimilation and atmospheric CO_2 inversions, the interannual variability in the air–sea CO_2 flux in the

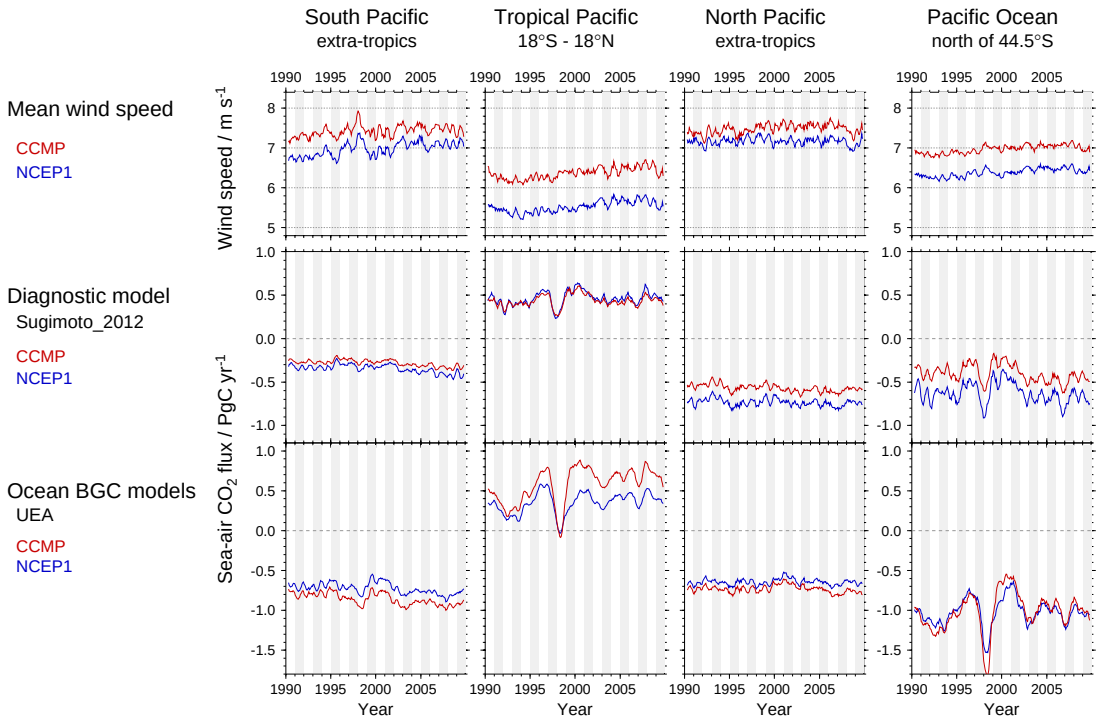

Fig. 10. Trend (5-month running means) of the Southern Oscillation Index (SOI) (http://ds.data.jma.go.jp/tcc/tcc/products/elnino/index/), and the air–sea CO_2 flux anomalies over the Pacific (44.5° S–66° N; black), in the tropical Pacific (18° S–18° N; red), in the North Pacific extratropics (18° N–18° S; blue), and in the South Pacific extratropics (green).

tropical zone is also large, but the effect of ENSO events is less clear.

6 Discussion

6.1 Dependence of air–sea CO_2 flux on wind product

The accuracy of wind field products over the ocean is fundamental to evaluating air–sea CO_2 fluxes in all approaches considered in this study. In atmospheric CO_2 inversions, the wind field directly controls the transport of CO_2. The wind field in the marine boundary layer is also required to drive ocean circulation in the prognostic OBGCMs, the pCO_2sw data assimilation, and the ocean-interior CO_2 inversions. In addition, various gas transfer velocities for CO_2 at the air–sea interface have been given empirically as a function of wind speed at 10m above sea surface and are needed to calculate air–sea CO_2 flux from the diagnostic models, forward OBGCMs and pCO_2sw data assimilation. Several wind products are available and have been used for these purposes. They include NCEP/NCAR Reanalysis 1 (Kalnay et al., 2007), NCEP/DOE Reanalysis 2 (Kanamitsu et al., 2002), ECMWF 40 Year Re-analysis (Uppala et al., 2005), JMA-CRIEPI JRA25/JCDAS (Onogi et al., 2007), and JPL CCMP Ocean Surface Wind Product (Ardizzone et al., 2009; Atlas et al., 2011). However, it is unclear how the choice of these wind products influences the resultant estimate of air–sea CO_2 fluxes, since a model is usually run with a single wind product and no comprehensive intercomparison exercise has been made in terms of the difference in the wind fields.

In this section, we briefly describe the impact of the difference in wind products on the estimates of air–sea CO_2 flux for a diagnostic model (Sugimoto et al., 2012) and an OBGCM (Buitenhuis et al., 2010). The wind products used here are NCEP/NCAR Reanalysis 1 (NCEP1), which has been often used to force the forward ocean models, and JPL CCMP Ocean Surface Wind Components (CCMP) that we used to calculate the air–sea CO_2 flux with the LDEO V2009 climatological pCO_2sw and with pCO_2sw diagnostic models in this work. In the diagnostic models, the gas transfer velocity for CO_2 that was applied in Eq.(1) with the CCMP wind product has a functional form that depends on the monthly mean second moment of wind speed $\langle U^2 \rangle$ and an empirical coefficient of 0.25. On the other hand, monthly mean wind speed squared, $\langle U \rangle^2$, and the coefficient 0.39 has been applied to the CO_2 gas transfer velocity of Wanninkhof (1992) with the NCEP1 wind product. In the OBGCM, daily wind speed and a coefficient appropriate for short-term wind speed of 0.3 has been applied with both wind products.

Mean seasonal variations and deseasonalized trends of regional mean wind speed, regionally integrated air–sea CO_2

flux from a diagnostic model (Sugimoto et al., 2012) and that from a OBGCM (Buitenhuis et al., 2010) are shown in Figs. 11 and 12 for each sub-basin of the Pacific Ocean. The seasonality in the regional mean wind speed in the extratropics, i.e., stronger in winter and weaker in summer, is clearly seen in Fig. 11. For the interannual variability in regional mean wind speed (Fig. 12), a positive anomaly in 1997–1998 in the South Pacific and a trend towards increasing wind speed in the South and tropical Pacific are observed. It is also evident that the mean wind speed in CCMP is always stronger than that in NCEP1. The difference is larger in the tropics (18° S–18° N) than in the extratropics. In the tropical Pacific,the monthly mean wind speed from CCMP and from NCEP1 varied in parallel to each other, and the time-averaged wind speed over the period 1990–2008 was $6.4\,m\,s^{-1}$ in CCMP and $5.5\,m\,s^{-1}$ in NCEP1. In the North Pacific extratropics, no significant difference was seen in the regional mean wind speed in early summer (May–July). However, in winter (December–February), mean CCMP wind speed ($8.9\,m\,s^{-1}$) is $0.6\,m\,s^{-1}$ stronger than that of NCEP1.

The difference in wind field influences the estimate of air–sea CO_2 fluxes from the diagnostic model and the forward ocean model in different ways. In the diagnostic modeling of Sugimoto et al. (2012), the air–sea CO_2 flux in the tropical Pacific calculated with the stronger CCMP wind field and that calculated with the weaker NCEP1 wind field agreed well both in the mean flux and in temporal variability (see Figs. 11 and 12). In spite of the large difference in the mean wind speed between CCMP and NCEP1, the difference in the air–sea CO_2 flux estimates was no more than $0.02\,Pg\,C\,yr^{-1}$ on average. This result indicates that the different formulations and coefficients of proportionality for CCMP and for NCEP1 in gas transfer velocity that have been individually calibrated with the bomb ^{14}C inventory in the global ocean successfully helped to account for the difference in the wind fields in the tropical Pacific. However, in the North and South Pacific extratropics, the weaker wind field of NCEP1 rather yielded stronger CO_2 sinks than the stronger wind field of CCMP. The differences are $0.07\,Pg\,C\,yr^{-1}$ for the South Pacific extratropics, $0.17\,Pg\,C\,yr^{-1}$ for the North Pacific extratropics, and $0.23\,Pg\,C\,yr^{-1}$ when integrated over the subbasins of the Pacific. These differences in the estimate of regional air–sea CO_2 fluxes due to the use of different combinations of wind field and gas transfer velocity are comparable to, and therefore, may explain a large part of the difference in the estimate between diagnostic models and OBGCMs (Table 4 and Fig. 6) in the extratropics and in the entire Pacific.

In contrast, the OBGCM of Buitenhuis et al. (2010) that has been forced with the stronger winds of CCMP (Table 2) yielded a stronger CO_2 source in the tropical Pacific and stronger sinks in the extratropics than that forced with the weaker winds of NCEP1. The magnitude of interannual variability in CO_2 outgassing in the tropical Pacific is also greater when the CCMP wind field was used to force the ocean model. The difference in the integrated CO_2 outflux amounted to $0.22\,Pg\,C\,yr^{-1}$ in the tropical Pacific, and the differences in the integrated CO_2 sinks in the extratropics amounted to $0.13\,Pg\,C\,yr^{-1}$ in the South Pacific and $0.09\,Pg\,C\,yr^{-1}$ in the North Pacific. Moreover, it is interesting to note that these differences are offsetting between the tropical source and extratropical sinks, and consequently the difference in the flux estimate integrated over the Pacific subbasins is minor ($< 0.02\,Pg\,C\,yr^{-1}$).

Importantly, the sensitivity described here for one forward OBGCM is likely due to different responses of the subtropical cell overturning to the wind stress component of forcing. For example, if the subtropical overturning strength were to be determined by the strength of the trade winds across 12° N and 12° S, the differences in zonal wind stress at these latitudes could sustain differences in the overturning strength of the subtropical cells, and as a linear advection issue the supply of carbon in the upwelling cold tongue. This may also find expression in increased subduction rates in the extratropical source regions, as illustrated by Fig. 1 of Rodgers et al. (2003). The response of simulated fields of DIC and pCO_2sw to the different wind forcing would of course vary from OBGCM to OBGCM. However, the results from this model suggest that the smaller CO_2 efflux from the tropical Pacific estimated by the forward OBGCMs than by the diagnostic models (Table 4 and Fig. 6) may reflect not only difference in winds used for calculating gas exchange, but also biases in the dynamical component of the wind forcing for the forward models (surface wind stress).

6.2 The "best estimates" of air–sea CO_2 flux in the Pacific regions

A focus of this effort was to obtain "best estimates" of time-averaged net air–sea CO_2 flux in each of the three sub-basins as well as over the entirety of the Pacific Basin by synthesizing the estimates from a variety of approaches. However, it is now clear that the synthesis of the estimates for the air–sea CO_2 flux in the Pacific Ocean does not provide a robust or convincing quantitative path to define a "best estimate". Rather, this synthesis exercise has provided an important first step towards assembling the information that will be needed for future efforts to construct a best estimate.

A quantitative assessment building on the results presented here would certainly require skill weighting in the construction of a model-mean or a model-median value of the air–sea CO_2 flux. Although this type of quantitative effort will not be conducted here, we can make loose use of the expression "best estimate" to describe a flux diagnostic that is consistent with what is calculated with the other RECCAP efforts for the Atlantic and Arctic Ocean basins (Schuster et al., 2013). This "best estimate" for the air–sea CO_2 flux is taken as the average of the results from (a) the diagnostic models and (b) the ocean-interior CO_2 inversions. Both of these approaches are anchored in observational constraints,

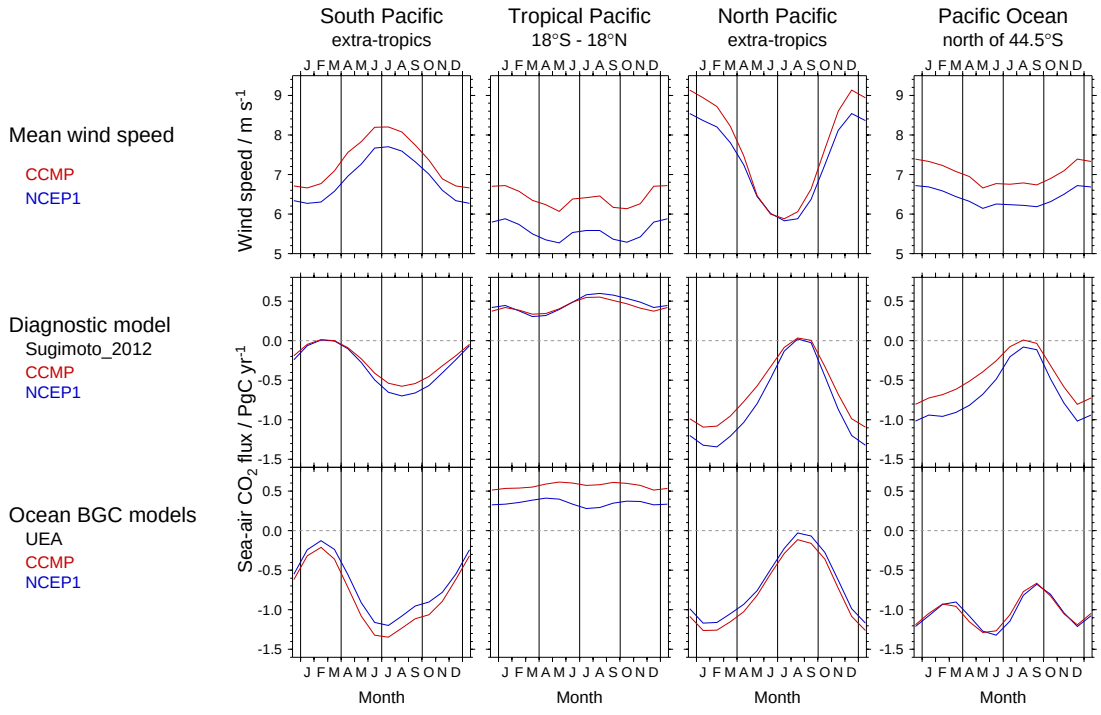

Fig. 11. Mean monthly wind speed of NCEP/NCAR Reanalysis 1 (NCEP1) (Kalnay et al., 2007) and Cross-Calibrated, Multi-Platform (CCMP) Ocean Surface Wind Product (http://podaac.jpl.nasa.gov/DATA_CATALOG/ccmpinfo.html) (Ardizzone et al., 2009; Atlas et al., 2011) (top), mean monthly air–sea CO_2 flux for 1990–2009 calculated with the diagnostic model of Sugimoto et al. (2012) (middle), and with the ocean biogeochemistry/general circulation model of Buitenhuis et al. (2010) (bottom) using the surface wind fields of NCEP1 and CCMP in the South Pacific extratropics (left), in the tropical Pacific (middle-left), in the North Pacific extratropics (middle-right), and in the entire Pacific region shown in Fig. 5.

with the data sources used by these two approaches being independent. As such, this "best estimate" is a simple average of the results obtained with surface pCO_2sw constraints and results obtained with ocean-interior tracer constraints. The uncertainty is then calculated from the uncertainties of the estimate from the diagnostic models (σ_{dia}) and ocean CO_2 inversions ($\sigma_{\mathrm{ocn\_inv}}$) as $\left\{(1/2)^2 \cdot \sigma^2_{\mathrm{dia}} + (1/2)^2 \cdot \sigma^2_{\mathrm{ocn\_inv}}\right\}^{1/2}$. Given the large uncertainty inherent in the gas transfer velocity calculated from the wind speed products, the uncertainty in the air–sea CO_2 flux from the diagnostic models (σ_{dia}) was assumed to be 50 % of the flux (Wanninkhof et al., 2013). The estimates thus appraised are examined for consistency with the results from OBGCMs. For comparison with the estimates here, the riverine CO_2 flux, $+0.08\,\mathrm{Pg\,C\,yr^{-1}}$ in the North Pacific extratropics and $+0.04\,\mathrm{Pg\,C\,yr^{-1}}$ in the tropical Pacific (Jacobson et al., 2007), are added to the results for six of eight OBGCMs in which riverine carbon discharge has not been taken into account (Table 2), and median ± MAD of flux estimates from all eight OBGCMs were recalculated.

In the North Pacific extratropics, the "best estimate" thus calculated is $-0.47 \pm 0.13\,\mathrm{Pg\,C\,yr^{-1}}$. This is consistent with the estimates from the OBGCMs ($-0.49 \pm 0.02\,\mathrm{Pg\,C\,yr^{-1}}$) (Table 4). Good consistency is also seen for the tropical Pacific where the "best estimate" is $+0.44 \pm 0.14\,\mathrm{Pg\,C\,yr^{-1}}$ and the median of the estimates from the OBGCMs is $+0.41 \pm 0.05\,\mathrm{Pg\,C\,yr^{-1}}$. In the South Pacific extratropics, the difference in the estimate of air–sea CO_2 flux between the diagnostic models and ocean-interior CO_2 inversions is larger ($0.18\,\mathrm{Pg\,C\,yr^{-1}}$) than those in other regions (0.10 to $0.15\,\mathrm{Pg\,C\,yr^{-1}}$). The variation in the estimates among different OBGCMs ($-0.39 \pm 0.11\,\mathrm{Pg\,C\,yr^{-1}}$) is also large. However, the mean of the estimates from the diagnostic models and ocean-interior CO_2 inversions ($-0.37 \pm 0.08\,\mathrm{Pg\,C\,yr^{-1}}$) is comparable to the estimate from the OBGCMs ($-0.39 \pm 0.11\,\mathrm{Pg\,C\,yr^{-1}}$). Finally, the "best estimate" of air–sea CO_2 flux for the entire Pacific basin north of 44.5° S ($-0.40 \pm 0.21\,\mathrm{Pg\,C\,yr^{-1}}$) was estimated from the results of diagnostic models ($-0.27 \pm 0.38\,\mathrm{Pg\,C\,yr^{-1}}$) and ocean-interior CO_2 inversions ($-0.52 \pm 0.18\,\mathrm{Pg\,C\,yr^{-1}}$). Given the quite large uncertainties and discrepancies between these estimates, it was not possible to obtain estimates with small uncertainty. The estimate for the entire Pacific Ocean basin is in reasonable agreement with the sum of the estimates from the OBGCMs after adding the riverine CO_2 flux ($-0.45 \pm 0.18\,\mathrm{Pg\,C\,yr^{-1}}$).

Absolutely critical to future efforts to reduce uncertainty in estimating the Pacific carbon sink will be future expansion of

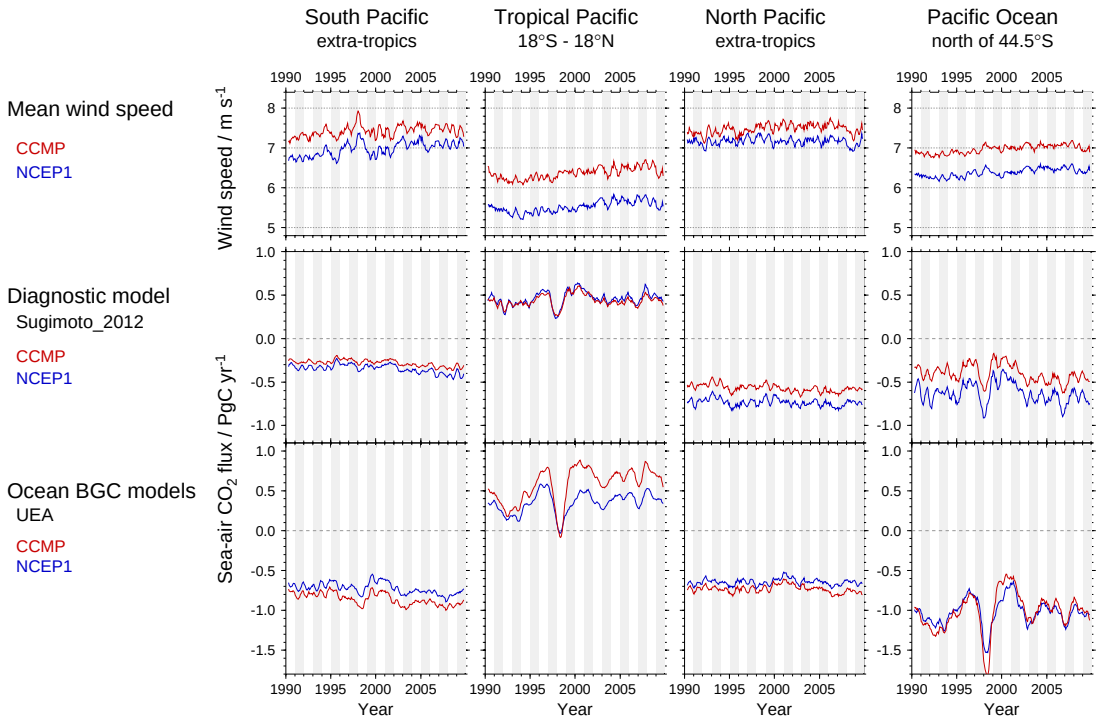

Fig. 12. Trend (5-month running means) of the monthly anomalies of wind speed of NCEP/NCAR Reanalysis 1 (NCEP1) (Kalnay et al., 2007) and Cross-Calibrated, Multi-Platform (CCMP) Ocean Surface Wind Product (http://podaac.jpl.nasa.gov/DATA_CATALOG/ccmpinfo.html) (Ardizzone et al., 2009; Atlas et al., 2011) (top), air–sea CO_2 flux for 1990–2009 calculated with the diagnostic model of Sugimoto et al. (2012) (middle), and with the ocean biogeochemistry/general circulation model of Buitenhuis et al. (2010) (bottom) using the surface wind fields of NCEP1 and CCMP in the South Pacific extratropics (45–18° S) (left), in the tropical Pacific (middle-left), in the North Pacific extratropics (18–66° N) (middle-right), and in the entire Pacific region shown in Fig. 5.

the ocean carbon observing system. As we have seen through our synthesis, two central priorities in expanding the observing system should be improving our characterization of seasonal variability and more extensive data sampling of the South Pacific. For a pCO_2sw-based flux estimate, an important component of efforts to better estimate CO_2 uptake will involve the combined use of sea surface pCO_2 measurements and diagnostic modeling. Similarly, it will be important to continue collection of hydrographic measurements of CO_2 chemistry given not only their intrinsic value but also their value to ocean inversion efforts. For both cases, the combined data/model analysis in the future will benefit greatly from the implementation and operation of autonomous platforms such as profiling floats and wave gliders mounted with the emerging technology of CO_2 and biogeochemical sensors (e.g., Martz et al., 2010; Fiedler et al, 2012). The autonomous platforms will certainly require coordinated efforts with the accurate measurements and calibration that are provided only by hydrographic measurements from research on oceanographic cruises. Additional measurements can be provided by efforts on voluntary observing ships. It is especially important that measurements are extended to fill in the data gaps in the Pacific Ocean with well-considered and planned sampling strategies (e.g., Lenton et al. 2009), particularly in the Southern Hemisphere, and in the seasonal variability.

In addition to the aforementioned monitoring efforts, prognostic ocean modeling will also play an important role in the continued development of process-understanding of the controls on physical-biogeochemical coupling in the ocean. As prognostic ocean models are also the basis of both ocean inversion studies and ocean biogeochemical assimilation efforts, they will directly benefit from better process representation in the models used for ocean carbon inversions. As was seen in Fig. 6, the largest discrepancies among the simulations with OBGCMs were found in the South Pacific. We will not identify the underlying cause of the discrepancies in detail within the context of this synthesis, but such discrepancies can result from differences in ocean model resolution, ocean physical parameterizations, and the representation of ocean biogeochemical processes. As was seen with the UEA model, important differences can also arise from differences in surface forcing fields.

7 Conclusions

In this study, a synthesis has been conducted of available observational products and modeling efforts to characterize the air–sea CO_2 fluxes over the Pacific Ocean basin. Consideration has been given to three regions, namely the extratropical North Pacific, the tropical Pacific, and the extratropical South Pacific. Consideration has also been given not only to the time–mean fluxes, but also to seasonal variability and interannual variability. With regard to the time-averaged air–sea CO_2 flux for 1990–2009, the estimates from all approaches are consistent in the sign of the flux for the tropical Pacific (efflux) as well as for the extratropics of the North and South Pacific (influx) (Table 4 and Fig. 6). In a considerable number of cases, the regional estimates agree within $0.1\,\mathrm{Pg\,C\,yr^{-1}}$. Some larger discrepancies are also seen between different approaches as well as among different models within the same approach.

In the tropical Pacific, time-averaged air–sea CO_2 fluxes for 1990–2009 from ocean-interior CO_2 inversions ($+0.37 \pm 0.12\,\mathrm{Pg\,C\,yr^{-1}}$) and OBGCMs ($+0.39 \pm 0.04\,\mathrm{Pg\,C\,yr^{-1}}$) agree well, but they are smaller than estimates derived from $p\mathrm{CO_2sw}$ diagnostic models ($+0.52 \pm 0.25\,\mathrm{Pg\,C\,yr^{-1}}$). Nevertheless, the differences are not significant if we consider the 50% flux uncertainty associated with the gas exchange coefficient and undersampling (Wanninkhof et al., 2013). Since the wind speed in the tropical Pacific has a quite large offset ($\sim 1\,\mathrm{m\,s^{-1}}$) among the wind products and the estimate of air–sea CO_2 flux from OBGCMs is considered to be sensitive to the choice of wind product that forces the model, the improvement of wind-speed products could be one of the key issues in reconciling the discrepancies in the flux estimate among these models. For the interannual variability, its peak-to-peak amplitude in the OBGCMs ($0.40 \pm 0.09\,\mathrm{Pg\,C\,yr^{-1}}$) is larger than that of diagnostic models ($0.27 \pm 0.07\,\mathrm{Pg\,C\,yr^{-1}}$). The amplitude is also sensitive to the choice of wind product in the OBGCMs. The skill of the diagnostic models that potentially underestimate interannual variability also needs further examinations.

In the North Pacific extratropics, where $p\mathrm{CO_2sw}$ diagnostic models and ocean-interior CO_2 inversions are relatively well constrained by the data of $p\mathrm{CO_2sw}$ and ocean-interior DIC, the agreement of time-averaged air–sea CO_2 fluxes over 1990–2009 between these approaches ($-0.52 \pm 0.25\,\mathrm{Pg\,C\,yr^{-1}}$ and $-0.42 \pm 0.08\,\mathrm{Pg\,C\,yr^{-1}}$) is fair. The estimates from OBGCMs ($-0.57 \pm 0.02\,\mathrm{Pg\,C\,yr^{-1}}$) were more negative, but become consistent with the other two approaches when riverine flux ($+0.08\,\mathrm{Pg\,C\,yr^{-1}}$) is added to the estimate. By contrast, the South Pacific extratropics remain severely undersampled for $p\mathrm{CO_2sw}$ and ocean-interior DIC. The discrepancy in the time-averaged air–sea CO_2 fluxes inferred from the $p\mathrm{CO_2sw}$ diagnostic model ($-0.28 \pm 0.13\,\mathrm{Pg\,C\,yr^{-1}}$) and ocean-interior CO_2 inversions ($-0.46 \pm 0.10\,\mathrm{Pg\,C\,yr^{-1}}$) is larger than in the North Pacific. The discrepancy needs to be reconciled in the future primarily through the increase in measurements both at the surface and in the interior of the ocean. The development of an improved observation network that incorporates deployments of autonomous instruments with CO_2 and biogeochemical sensors has a great potential to contribute to filling in the data gaps in the Pacific Ocean, particularly in the Southern Hemisphere. The estimate from the OBGCMs ($-0.39 \pm 0.11\,\mathrm{Pg\,C\,yr^{-1}}$) in the South Pacific extratropics is rather consistent with the estimate from ocean-interior CO_2 inversions, but its uncertainty is greater than twice that in other sub-basins of the Pacific Ocean. The causes of such a large variation among OBGCMs in the South Pacific extratropics are yet to be clarified.

For the entire Pacific Ocean between 44.5° S and 66°N, the time-averaged net air–sea CO_2 flux for 1990–2009 is $-0.27 \pm 0.38\,\mathrm{Pg\,C\,yr^{-1}}$ from $p\mathrm{CO_2sw}$ diagnostic models, $-0.52 \pm 0.18\,\mathrm{Pg\,C\,yr^{-1}}$ from ocean-interior CO_2 inversions, and $-0.57 \pm 0.12\,\mathrm{Pg\,C\,yr^{-1}}$ from the OBGCMs. The discrepancies in the estimates in the sub-basins of the Pacific between the diagnostic models and other two approaches were reinforced when integrated over the Pacific Ocean. On the other hand, the diagnostic models and OBGCMs are consistent with each other in that the interannual variability in the air–sea CO_2 flux in the Pacific Ocean is dominated by the interannual variability in the tropical zone and is associated with the ENSO events.

The model with $p\mathrm{CO_2sw}$ data assimilation gave the smallest efflux in the tropics ($+0.27\,\mathrm{Pg\,C\,yr^{-1}}$) and the smallest influx into the extratropics of the North Pacific ($-0.37\,\mathrm{Pg\,C\,yr^{-1}}$) and the South Pacific ($-0.24\,\mathrm{Pg\,C\,yr^{-1}}$) among the approaches considered in this study. The phase of interannual variability in the tropics is not always consistent with the results from diagnostic models and OBGCMs.

Atmospheric CO_2 inversions gave the largest variety of estimates of time-averaged air–sea CO_2 flux in each of the North Pacific extratropics ($-0.48 \pm 0.08\,\mathrm{Pg\,C\,yr^{-1}}$), tropics ($-0.53 \pm 0.08\,\mathrm{Pg\,C\,yr^{-1}}$), and the South Pacific extratropics ($-0.29 \pm 0.08\,\mathrm{Pg\,C\,yr^{-1}}$). The median of the estimates is fairly consistent with the estimate from the LDEO V2009 climatological $p\mathrm{CO_2sw}$ and $p\mathrm{CO_2sw}$ diagnostic models, possibly because of the use of the climatological CO_2 flux from $p\mathrm{CO_2sw}$ in the flux priors.

Appendix A

Decadal mean air–sea CO_2 fluxes

Regionally integrated and time-averaged net air–sea CO_2 flux ($\mathrm{Pg\,C\,yr^{-1}}$) for 1990–1999 and 2000–2009 in the Pacific Ocean regions from various approaches are shown in Table A1.

Table A1. Decadal mean values of the regionally integrated air–sea CO_2 flux in three sub-basins of the Pacific Ocean evaluated from various approaches. All units are Pg C yr^{-1}.

Regions [Area (km^2)]	Period	pCO_2sw Diag. Models[1]	Ocean Inv.[2]	OBGC Models[3]	pCO_2sw Data Assim.[4]	Atm. Inv.[3,4]
North Pacific extratropics	1990–1999	-0.51 ± 0.03	-0.42 ± 0.08	-0.58 ± 0.03	-0.37	-0.44 ± 0.08
66–18° N	2000–2009	-0.53 ± 0.07	-0.42 ± 0.08	-0.57 ± 0.02	-0.36	-0.53 ± 0.07
[4.43×10^7]						
Tropical Pacific	1990–1999	$+0.49 \pm 0.07$	$+0.37 \pm 0.12$	$+0.36 \pm 0.06$	$+0.27$	$+0.53 \pm 0.07$
18° N–18° S						
[6.65×10^7]	2000–2009	$+0.56 \pm 0.11$	$+0.36 \pm 0.12$	$+0.41 \pm 0.04$	$+0.28$	$+0.54 \pm 0.07$
South Pacific extratropics	1990–1999	-0.27 ± 0.01	-0.46 ± 0.10	-0.38 ± 0.11	-0.23	-0.26 ± 0.09
18–44.5° S	2000–2009	-0.29 ± 0.01	-0.46 ± 0.10	-0.40 ± 0.12	-0.24	-0.29 ± 0.07
[3.88×10^7]						
All Pacific	1990–1999	-0.29 ± 0.08	-0.51 ± 0.18	-0.61 ± 0.12	-0.34	-0.22 ± 0.17
66° N–44.5° S						
[14.96×10^7]	2000–2009	-0.25 ± 0.18	-0.52 ± 0.18	-0.53 ± 0.13	-0.33	-0.35 ± 0.07

[1] Mean ± half of range of two diagnostic models of Park et al. (2010) and Sugimoto et al. (2012).
[2] Skill-weighted average ± standard deviation of the ocean CO_2 inversions.
[3] Median ± median absolute deviation of estimates from various models and inversions.
[4] For the period 1990–2008.

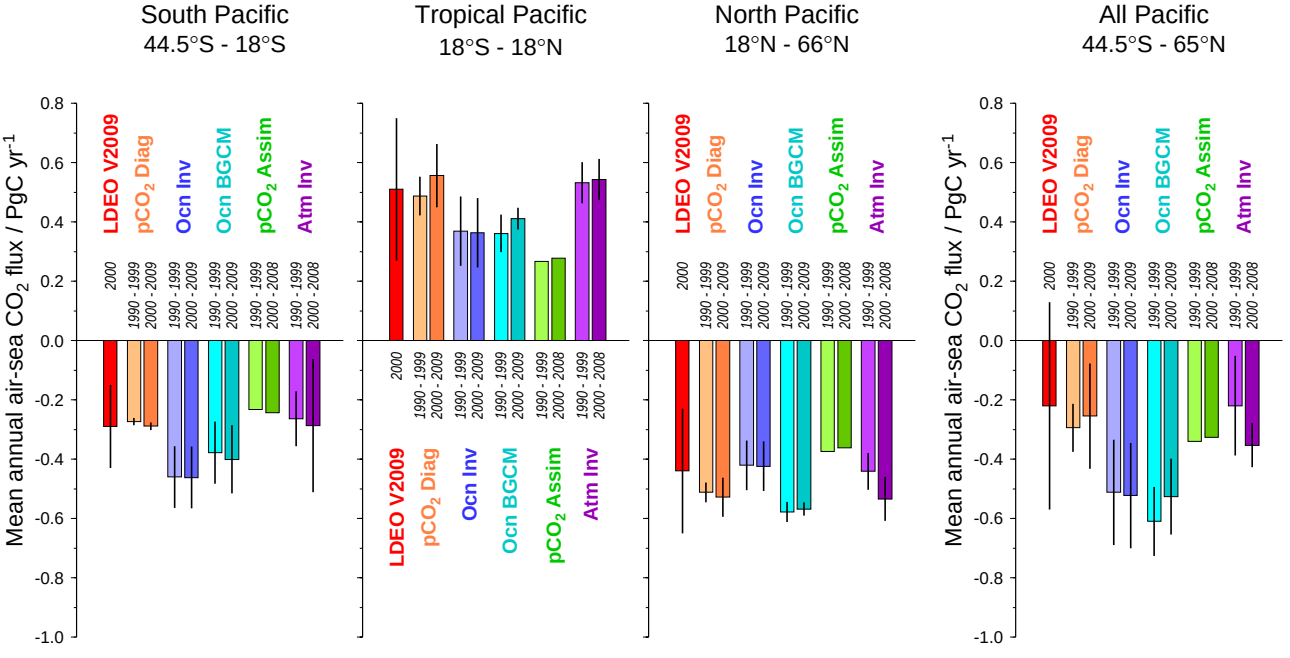

Fig. A1. Summary of regionally integrated and time-averaged net air–sea CO_2 flux (Pg C yr^{-1}) for 1990–1999 and 2000–2009 in the Pacific Ocean regions shown in Fig. 5.

Acknowledgements. This work has been done as one of the synthesis efforts of the project Regional Carbon Cycle Assessment and Processes (RECCAP) of Global Carbon Project. We thank J. G. Canadell, P. Ciais, C. Le Quéré, and C. Sabine for coordinating the RECCAP, and F. Perez and an anonymous reviewer for constructive suggestions to this manuscript. We also thank the captains, officers, and crew of all the many ships on which carbon measurements have been made and contributed to this work. All the modelers' contribution by providing the data sets of their model runs are also much appreciated. The OBGCM results are provided in RECCAP OBGCM site at http://lgmacweb.env.uea.ac.uk/lequere/reccap/. We thank the Bjerknes Centre for Climate Research (University of Bergen and Uni Research AS) for providing data of the MICOM-HAMOCC model and ETH Zurich for providing the data of NCAR CCSM3 ocean model with BEC with the gas exchange formulation of global mean velocity of 15 cm h^{-1} for CO_2 (ETHk15). The inverse model results of atmospheric CO_2 are provided under TransCom project at http://transcom.lsce.ipsl.fr. The data sets of CCMP Ocean Surface Wind Product are provided from Physical Oceanography Distributed Active Archive Center of NASA Jet Propulsion Laboratory, and the data sets of wind speed of NCEP/NCAR Reanalysis 1 are provided from CSIL Research Data Archive managed by NCAR's Data Support Section. M. Ishii acknowledges the Meteorological Research Institute's priority research fund for ocean carbon cycle changes, JSPS Grant-in-Aid for Scientific Research (B) No. 22310017, and MEXT Grant-in-Aid for Scientific Research on Innovative Areas No. 24121003. Support for K. B. Rodgers came under awards NA17RJ2612 and NA08OAR4320752, and support for K. B. Rodgers and R. A. Feely from the NOAA Office of Oceanic and Atmospheric Research (OAR) through the office of Climate Observations (OCO), as well as by funds from NASA's Research Opportunities in Space and Earth Sciences through award #NNX09AI13G. SMF's contributions were funded through the NIWA National Centre for Atmosphere's core research funding. S. C. Doney and I. Lima acknowledge support from US National Science Foundation award AGS-1048827. E. T. Buitenhuis acknowledges support from the EU (CarboChange, contract 264879). A. Lenton acknowledges support from the Australian Climate Change Science Program. T. Takahashi is supported by grants from the NOAA (NA08OAR4320754) and the Comer Science and Education Foundation (CSEF CP70).

Edited by: J. Canadell

References

Ardizzone, J., Atlas, R., Hoffman, R. N., Jusem, J. C., Leidner, S. M., and Moroni, D. F.: New multiplatform ocean surface wind product available, EOS Trans., 90, p. 231, 2009.

Assmann, K. M., Bentsen, M., Segschneider, J., and Heinze, C.: An isopycnic ocean carbon cycle model, Geosci. Model Dev., 3, 143–167, doi:10.5194/gmd-3-143-2010, 2010.

Atlas, R., Hoffman, R. N., Ardizzone, J., Leidner, S. M., Jusem, J. C., Smith, D. K., and Gombos, D.: A cross-calibrated multiplatform ocean surface wind velocity product for meteorological and oceanographic applications, B. Am. Meteor. Soc., 92, 157–174, doi:10.1175/2010BAMS2946.1, 2011.

Aumont, O. and Bopp, L.: Globalizing results from ocean in situ iron fertilization studies, Global Biogeochem. Cy., 20, GB2017, doi:10.1029/2005GB002591, 2006.

Baker, D. F., Law, R. M., Gurney, K. R., Rayner, P., Peylin, P., Denning, A. S., Bousquet, P., Bruhwiler, L., Chen, Y. H., Ciais, P., Fung, I. Y., Heimann, M., John, J., Maki, T., Maksyutov, S., Masarie, K., Prather, M., Pak, B., Taguchi, S., and Zhu, Z.: TransCom 3 inversion intercomparison: Impact of transport model errors on the interannual variability of regional CO_2 fluxes, 1988–2003, Global Biogeochem. Cy., 20, GB1002, doi:10.1029/2004gb002439, 2006.

Buitenhuis, E. T., Rivkin, R. B., Sailley, S., and Le Quere, C.: Biogeochemical fluxes through microzooplankton, Global Biogeochem. Cy., 24, GB4015, doi:10.1029/2009GB003601, 2010.

Canadell, J. G., Ciais, P., Gurney, K., Le Quéré, C., Piao, S., Raupach, M. R., and Sabine, C.: An international effort to to quantify regional carbon fluxes, EOS, 92, 81–82, doi:10.1029/2011EO100001, 2011.

Chevallier, F., Ciais, P., Conway, T. J., Aalto, T., Anderson, B. E., Bousquet, P., Brunke, E. G., Ciattaglia, L., Esaki, Y., Frohlich, M., Gomez, A., Gomez-Pelaez, A. J., Haszpra, L., Krummel, P. B., Langenfelds, R. L., Leuenberger, M., Machida, T., Maignan, F., Matsueda, H., Morgui, J. A., Mukai, H., Nakazawa, T., Peylin, P., Ramonet, M., Rivier, L., Sawa, Y., Schmidt, M., Steele, L. P., Vay, S. A., Vermeulen, A. T., Wofsy, S., and Worthy, D.: CO_2 surface fluxes at grid point scale estimated from a global 21 year reanalysis of atmospheric measurements, J. Geophys. Res., 115, D21307, doi:10.1029/2010jd013887, 2010.

Chierici, M., Fransson, A., and Nojiri Y.: Biogeochemical processes as drivers of surface fCO_2 in contrasting provinces in the subarctic North Pacific Ocean, Global Biogeochem. Cy., 20, GB1009, doi:10.1029/2004GB002356, 2006.

Christian, J. R., Feely, R. A., Ishii, M., Murtugudde, R., and Wang, X.: Testing an ocean carbon model with observed sea surface pCO_2 and dissolved inorganic carbon in the tropical Pacific Ocean, J. Geophys. Res., 113, C07047, doi:10.1029/2007JC004428, 2008.

Doney, S. C., Lima, I., Feely, R. A., Glover, D. M., Lindsay, K., Mahowal, N., Moore, J. K., and Wanninkhof, R.: Mechanisms governing interannual variability in the upper ocean inorganic carbon system and air-sea CO_2 fluxes: Physical climate and atmospheric dust, Deep-Sea Res. II, 56, 640–655, doi:10.1016/j.dsr2.2008.12.006, 2009a.

Doney, S. C., Lima, I., Moore, J. K., Lindsay, K., Behrenfeld, M. J., Westberry, T. K., Mahowald, N., Glover, D. M., and Takahashi, T.: Skill metrics for confronting global upper ocean ecosystem biogeochemistry models against field and remote sensing data, J. Mar. Syst., 76, 95–112, doi:10.1016/j.jmarsys.2008.05.015, 2009b.

Dore, J., Lukas, R., Sadler, D. W., and Karl D. M.: Climate-driven changes to the atmospheric CO_2 sink in the subtropical North Pacific Ocean, Nature, 424, 754–757, doi:10.1038/nature01885, 2003.

Dore, J., Lukas, R., Sadler, D. W., Church, M. J., and Karl, D. M.: Physical and biogeochemical modulation of ocean acidification in the central North Pacific, P. Natl. Acad. Sci., 106, 12235–12240, doi:10.1073/pnas.0906044106, 2009.

Dunne, J. P., John, J. G., Adcroft, A. J., Griffies, S. M., Hallberg, R. W., Shevliakova, E., Stouffer, R. J., Cooke, W., Dunne, K.

A., Harrison, M. J., Krasting, J. P., Malyshev, S. L., Milly, P. C. D., Phillipps, P. J., Sentman, L. T., Samuels. B. L., Spelman, M. J., Winton, M., Wittenberg, A. W., and Zadeh, N.: GFDL's ESM2M global coupled climate-carbon Earth System Models Part I: Physical formulation and baseline simulation characteristics, J. Climate, 25, 6646–6665, doi:10.1175/JCLI-D-11-00560.1, 2012.

Feely, R. A., Gammon, R. H., Taft, B. A., Pullen, P. E., Waterman, L. S., Conway, T. H., Gendron, J. F., and Wisegarver, D. P.: Distribution of chemical tracers in the eastern equatorial pacific during and after the 1982–83 El Nino/Southern Oscillation Event, J. Geophys. Res. 92, 6545–6558, doi:10.1029/JC092iC06p06545, 1987.

Feely, R. A., Wanninkhof, R., Takahashi, T., and Tans, P.: Influence of El Niño on the equatorial Pacific contribution to atmospheric CO_2 accumulation, Nature, 398, 597–601, doi:10.1038/19273, 1999.

Feely, R.A., Boutin, J., Cosca, C. E., Dandonneau, Y., Etcheto, J., Inoue, H. Y., Ishii, M., Le Quéré, C., Mackey, D. J., McPhaden, M., Metzl, N., Poisson, A., and Wanninkhof, R.: Seasonal and interannual variability of CO_2 in the equatorial Pacific, Deep-Sea Res. II, 49, 2443–2469, 2002.

Feely, R. A., Takahashi, T., Wanninkhof, R., McPhaden, M. J., Cosca, C. E., Sutherland, S. C., and Carr M.-E.: Decadal variability of the air-sea CO_2 fluxes in the equatorial Pacific Ocean, J. Geophys. Res., 111, C08S90, doi:10.1029/2005JC003129, 2006.

Fiedler, B., Fietzek, P., Vieira, N., Silvia, P., Bittig, H. C., and Kortzinger, A.: In situ CO_2 and O_2 measurements on a profiling float, J. Atom. Ocean. Technol., 30, 112–126, doi:10.1175/JTECH-D-12-00043.1, 2013.

Gloor, M., Gruber, N., Sarmiento, J., Sabine, C. L., Feely, R. A., and Rödenbeck, C.: A first estimate of present and preindustrial air-sea CO_2 fluxes patterns based on ocean interior carbon measurements and models, Geophys. Res. Lett., 30, 1010, doi:10.1029/2002GL015594, 2003.

Gorgues, T., Aumont, O., and Rodgers, K. B.: A mechanistic account of increasing seasonal variations in the rate of ocean uptake of anthropogenic carbon, Biogeosciences, 7, 2581–2589, doi:10.5194/bg-7-2581-2010, 2010.

Graven, H. D., Gruber, N., Key, R., Khatiwala, S., and Giraud, X.: Changing controls on oceanic radiocarbon: New insights on shallow-to-deep ocean exchange and anthropogenic CO_2 uptake, J. Geophys. Res., 117, C10005, doi:10.1029/2012JC008074, 2012.

Gruber, N., Gloor, M., Mikaloff Fletcher, S. E., Doney, S. C., Dutkiewicz, S., Follows, M. J., Gerber, M., Jacobson, A. R., Joos, F., Lindsay, K., Menemenlis, D., Mouchet, A., Müller, S. A., Sarmiento, J. L., and Takahashi, T.: Oceanic sources, sinks, and transport of atmospheric CO_2, Global Biogeochem. Cy., 23, GB1005, doi:10.1029/2008GB003349, 2009.

Inoue, H., Sugimura, Y., and Fushimi, K.: pCO_2 and $\delta^{13}C$ in the air and surface water in the western North Pacific, Tellus B, 39, 228–242, doi:10.1111/j.1600-0889.1987.tb00285.x, 1987.

Inoue, H. Y. and Sugimura, Y.: Variations and distributions of CO_2 in and over the equatorial Pacific during the period from the 1986/88 El Niño event to the 1988/89 La Niña event, Tellus B, 44, 1–22, doi:10.1034/j.1600-0889.1992.00001.x, 1992.

Inoue, H. Y., Matsueda, H., Ishii, M., Fushimi, K., Hirota, M., Asanuma, I., and Takasugi Y.: Long-term trend of the partial pressure of carbon dioxide (pCO_2) in surface waters of the western North Pacific, 1984–1993, Tellus B, 47, 391–413, doi:10.1034/j.1600-0889.47.issue4.2.x,1995.

Inoue, H. Y., Ishii, M., Matsueda, H., Saito, S., Midorikawa, T., and Nemoto, K.: MRI measurements of partial pressure of CO_2 in surface waters of the Pacific during 1968 to 1970: re-evaluation and comparison of data with those of the 1980s and 1990s, Tellus B, 51, 830–848, doi:10.1034/j.1600-0889.1999.t01-3-00007.x, 1999.

Ishii, M. and Inoue, H. Y.: Air-sea exchange of CO_2 in the central and western equatorial Pacific in 1990, Tellus B, 47, 447–460, doi:10.1034/j.1600-0889.47.issue4.5.x, 1995.

Ishii, M., Inoue, H. Y., Matsueda, H., Saito, S., Fushimi, K., Nemoto, K., Yano, T., Nagai, H., and Midorikawa, T.: Seasonal variation in total inorganic carbon and its controlling processes in surface waters of the western North Pacific subtropical gyre, Mar. Chem., 75, 17–32, 2001.

Ishii, M., Saito, S., Tokieda, T., Kawano, T., Matsumoto, K., and Inoue, H. Y.: Variability of surface layer CO_2 parameters in the western and central equatorial Pacific, in: Global environmental change in the ocean and on land, edited by: Shiyomi, M., Kawahata, H., Koizumi, H., Tsuda, A., and Awaya, Y., Terrapub, Tokyo, 59–94, 2004.

Ishii, M., Inoue, H.Y., Midorikawa, T., Saito, S., Tokieda, T., Sasano, D., Nakadate, A., Nemoto, K., Metzl, N., Wong, C. S., and Feely, R. A.: Spatial variability and decadal trend of the oceanic CO_2 in the western equatorial Pacific warm/fresh water, Deep-Sea Res. II, 56, 591–606, doi:10.1016/j.dsr2.2009.01.002, 2009.

Jacobson, A. R., Mikaloff Fletcher, S. E., Gruber, N., Sarmiento, J. L., and Gloor, M.: A joint atmosphere-ocean inversion for surface fluxes of carbon dioxide: 1. Methods and global-scale fluxes, Global Biogeochem. Cy., 21, GB1019, doi:10.1029/2005GB002556, 2007.

Kalnay, E., Kanamitsu, M., Kistler, R., Collins, W., Deaven, D., Gandin, L., Iredell, M., Saha, S., White, G., Woollen, J., Zhu, Y., Leetmaa, A., Reynolds, R., Chelliah, M., Ebisuzaki, W., Higgins, W., Janowiak, J., Mo, K. C., Ropelewski, C., Wang, J., Jenne, R., and Joseph, D.: The NCEP/NCAR 40-year reanalysis project, B. Am. Meteor. Soc., 77, 437–470, 1996.

Kanamitsu, M., Ebisuzaki, W., Woollen, J., Yang, S.-K., Hnilo, J. J., Fiorino, M., and Potter, G. L.: NCEP-DOE AMIP-II Reanalysis (R-2), B. Am. Meteor. Soc., 83, 1631–1643, 2002.

Keeling, C. D., Brix, H., and Gruber, N.: Seasonal and long-term dynamics of the upper ocean carbon cycle at Station ALOHA near Hawaii, Global Biogeochem. Cy., 18, GB4006, doi:10.1029/2004GB002227, 2004.

Key, R. M., Kozyr, A., Sabine, C. L., Lee, K., Wanninkhof, R., Bullister, J. L., Feely, R. A., Millero, F. J., Mordy, C., and Peng, T.-H.: A global ocean carbon climatology: Results from Global Data Analysis Project (GLODAP), Global Biogeochem. Cy. 18, GB4031, doi:10.1029/2004GB002247, 2004.

Lee, K., Wanninkhof, R., Takahashi, T., Doney, S. C., and Feely, R. A.: Low interannual variability in recent oceanic uptake of atmospheric carbon dioxide, Nature, 396, 155–159, doi:10.1038/24139, 1998.

Lee, K., Tong, L. T., Millero, F. J., Sabine, C. L., Dickson, A. G., Goyet, C., Park, G.-H., Wanninkhof, R., Feely, R. A., and Key, R. M.: Global relationships of total alkalinity with salinity and tem-

perature in surface waters of the world's oceans, Geophy. Res. Lett., 33, L19605, doi:10.1029/2006GL027207, 2006.

Lenton, A., Bopp, L., and Matear, R. J.: Strategies for high-latitude northern hemisphere CO_2 sampling now and in the future, Deep-Sea Res. II, 56, 523–532, doi:10.1016/j.dsr2.2008.12.008, 2009.

Lenton, A., Metzl, N.,Takahashi, T., Kuchinke, M., Matear, R. J., Roy, T., Sutherland, S. C., Sweeney, C., and Tilbrook, B.: The observed evolution of oceanic pCO_2 and its drivers over the last two decades, Global Biogeochem. Cy., 26, GB2021, doi:10.1029/2011GB004095, 2012.

Lenton, A., Tilbrook, B., Law, R. M., Bakker, D., Doney, S. C., Gruber, N., Ishii, M., Hoppema, M., Lovenduski, N. S., Matear, R. J., McNeil, B. I., Metzl, N., Mikaloff Fletcher, S. E., Monteiro, P. M. S., Rödenbeck, C., Sweeney, C., and Takahashi, T.: Sea–air CO_2 fluxes in the Southern Ocean for the period 1990–2009, Biogeosciences, 10, 4037–4054, doi:10.5194/bg-10-4037-2013, 2013.

Le Quéré, C., Orr, J. C., Monfray, P., Aumont, O., and Madec, G.: Interannual variability of the oceanic sink of CO_2 from 1979 through 1997, Global Biogeochem. Cy., 14, 1247–1265, doi:10.1029/1999GB900049, 2000.

Loukos, H., Vivier, F., Murphy, P. P., Harrison, D. E., and Le Quéré, C.: Interannual variability of equatorial Pacific CO_2 fluxes estimated from temperature and salinity data, Geophys. Res. Lett., 27, 1735–1738, doi:10.1029/1999GL011013, 2000.

Maki, T., Ikegami, M., Fujita, T., Hirahara, T., Yamada, K., Mori, K., Takeuchi, A., Tsutsumi, Y., Suda, K., and Conway, T. J.: New technique to analyse global distributions of CO_2 concentrations and fluxes from non-processed observational data, Tellus B, 62, 797–809, doi:10.1111/J.1600-0889.2010.00488.X, 2010.

Mantua, N. J., Hare, S. R., Zhang, Y., Wallace, J. M., and Francis, R. C.: A Pacific interdecadal climate oscillation with impacts on salmon production, Bull. Amer. Meteor. Soc., 78, 1069–1079, 1997.

Martz, T. R., Connery, J. G., and Johnson, K. S.: Testing the Honeywell Durafet® for seawater pH applications, Limnol. Oceanogr.-Methods, 8, 172–184, doi:10.4319/lom.2010.8.172, 2010.

Matear, R. J. and Lenton, A.: Impact of historical climate change on the Southern Ocean carbon cycle, J. Climate, 21, 5820–5834, doi:10.1175/2008JCLI2194.1, 2008.

McKinley, G. A., Follows, M. J., and Marshall, J.: Mechanisms of air-sea CO_2 flux variability in the equatorial Pacific and the North Atlantic, Global Biogeochem. Cy., 18, GB2011, doi:10.1029/2003GB002179, 2004.

McKinley, G. A., Takahashi, T., Buitenhuis, E., Chai, F., Christian, J. R., Doney, S. C., Jiang, M.-S., Lindsay, K., Moore, J. K., Le Quéré,, C., Lima, I., Murtugudde, R., Shi, L., and Wetzel, P.: North Pacific carbon cycle response to climate variability on seasonal to decadal timescales, J. Geophys. Res., 111, C07S06, doi:10.1029/2005JC003173, 2006.

McPhaden, M. J. and Zhang, D.: Slowdown of the meridional overturning circulation in the upper Pacific Ocean, Nature, 415, 603–608, doi:10.1038/415603a, 2002.

McPhaden, M. J. and Zhang, D.: Pacific Ocean circulation rebounds. Geophys. Res. Lett., 31, L18301, doi:10.1029/2004GL020727, 2004.

Metzl, N., Tilbrook, B., and Poisson, A.: The annual fCO_2 cycle and the air-sea CO_2 flux in the sub-Antarctic Ocean, Tellus B, 51, 849–861, doi:10.1034/j.1600-0889.1999.t01-3-00008.x, 1999.

Midorikawa, T., Nemoto, K., Kamiya, H., Ishii, M., and Inoue, H. Y.: Persistently strong oceanic CO_2 sink in the western subtropical North Pacific, Geophys. Res. Lett., 32, L05612, doi:10.1029/2004GL021952, 2005.

Midorikawa,T., Ishii, M., Nemoto, K, Kamiya, H., Nakadate, A., Masuda, S., Matsueda, H., Nakano, T., and Inoue, H. Y.: Interannual variability of winter oceanic CO_2 and air-sea CO_2 flux in the western North Pacific for 2 decades, J. Geophys. Res., 111, C07S02, doi:10.1029/2005JC003095, 2006.

Midorikawa, T., Ishii, M., Kosugi, N., Sasano, D., Nakano, T., Saito, S., Sakamoto, N., Nakano, H., and Inoue, H. Y.: Recent deceleration of oceanic pCO_2 increase in the western North Pacific in winter, Geophys. Res. Lett., 39, L12601, doi:10.1029/2012GL051665, 2012.

Mikaloff Fletcher, S. E., Gruber, N., Jacobson, A. R., Doney, S. C., Dutkiewicz, S., Gerber, M., Follows, M., Joos, F., Lindsay, K., Menemenlis, D., Mouchet, A., Müller, S. A., and Sarmiento, J. L.: Inverse estimates of anthropogenic CO_2 uptake, transport, and storage by the ocean, Global Biogeochem. Cy., 20, GB2002, doi:10.1029/2005GB002530, 2006.

Mikaloff Fletcher, S. E., Gruber, N., Jacobson, A. R., Gloor, M., Doney, S. C., Dutkiewicz, S., Gerber, M., Follows, M., Joos, F., Lindsay, K., Menemenlis, D., Mouchet, A., Müller, S. A., and Sarmiento, J. L.: Inverse estimates of the oceanic sources and sinks of natural CO_2 and the implied oceanic carbon transport, Global Biogeochem. Cy., 21, GB1010, doi:10.1029/2006GB002751, 2007.

Nakano, H., Tsujino, H., Hirabara, M., Yasuda, T., Motoi, T., Ishii, M., and Yamanaka, G.: Uptake mechanism of anthropogenic CO_2 in the Kuroshio Extension region in an ocean general circulation model, J. Oceanogr., 67, 765–783, doi:10.1007/s10872-011-0075-7, 2011.

Nakaoka, S., Telszewski, M., Nojiri, Y., Yasunaka, S., Miyazaki, C., Mukai, H., and Usui, N.: Estimating temporal and spatial variation of ocean surface pCO_2 in the North Pacific using a self-organizing map neural network technique, Biogeosciences, 10, 6093–6106, doi:10.5194/bg-10-6093-2013, 2013.

Niwa, Y., Machida, T., Sawa, Y., Matsueda, H., Schuck, T. J., Brenninkmeijer, C. A. M., Imasu, R., and Satoh, M.: Imposing strong constraints on tropical terrestrial CO_2 fluxes using passenger aircraft based measurements, J. Geophys. Res., 117, D11303, doi:10.1029/2012jd017474, 2012.

Obata, A. and Kitamura, Y.: Interannual variability of the air-sea exchange of CO_2 from 1961 to 1998 simulated with a global ocean circulation-biogeochemistry model, J. Geophys. Res., 108, 3337, doi:10.1029/2001JC001088, 2003.

Onogi, K., Tsutsui, J., Koide, H., Sakamoto, M., Kobayashi, S., Hatsushika, H., Matsumoto, T., Yamazaki, N., Kamahori, H., Takahashi, K., Kadokura, S., Wada, K., Kato, K., Oyama, R., Ose, T., Mannoji, N., and Taira, R.: The JRA-25 Reanalysis, J. Meteor. Soc. Jpn., 85, 369–432, 2007.

Piao, S., Fang, J., Ciais, P., Peylin, P., Huang, Y., Sitch, S., and Wang, T.: The carbon balance of terrestrial ecosystems in China, Nature, 458, 1009–1013, doi:10.1038/nature07944, 2009.

Park, G.-H., Wanninkhof, R., Doney, S. C., Takahashi, T., Lee, K., Feely, R. A., Sabine, C. L., Trinanes, J., and Lima, I. D.: Variability of global net sea–air CO_2 fluxes over the last three decades using empirical relationships, Tellus B, 62, 352–368, doi:10.1111/j.1600-0889.2010.00498.x, 2010.

Park, G.-H. and Wanninkhof, R.: A large increase of the CO_2 sink in the western tropical North Atlantic from 2002 to 2009, J. Geophys. Res., 117, C08029, doi:10.1029/2011JC007803, 2012.

Patra, P. K., Maksyutov, S., Ishizawa, M., Nakazawa, T., Takahashi, T., and Ukita, J.: Interannual and decadal changes in the air-sea CO_2 flux from atmospheric CO_2 inverse modeling, Global Biogeochem. Cy., 19, GB4013, doi:10.1029/2004GB002257, 2005.

Peters, W., Jacobson, A. Sweeney, C., Andrews, A., Conway, T., Masarie, K., Miller, J. B., Bruhweiler, L. M. P., Pétron, G., Hirsh, A. I., Worth, D. E. J., van der Werf, G. R., Randerson, J. T., Wennberg, P. O., Krol, M. C., and Tans, P. P.: An atmospheric perspective on North American carbon dioxide exchange: Carbon Tracker, P. Natl. Acad. Sci., 104, 18925–18930, doi:10.1073/pnas.0708986104, 2007.

Peylin, P., Bousquet, P., Le Quéré, C., Sitch, S., Friedlingstein, P., McKinley, G., Gruber, N., Rayner, P., and Ciais, P.: Multiple constraints on regional CO_2 flux variations over land and oceans, Global Biogeochem. Cy., 19, GB1011, doi:10.1029/2003GB002214, 2005.

Peylin, P., Law, R. M., Gurney, K. R., Chevallier, F., Jacobson, A. R., Maki, T., Niwa, Y., Patra, P. K., Peters, W., Rayner, P. J., Rödenbeck, C., van der Laan-Luijkx, I. T., and Zhang, X.: Global atmospheric carbon budget: results from an ensemble of atmospheric CO_2 inversions, Biogeosciences, 10, 6699–6720, doi:10.5194/bg-10-6699-2013, 2013.

Qiu, B. and Chen, S.: Interannual-to-decadal variability in the bifurcation of the North Equatorial Current off the Philippines, J. Phys. Oceanogr., 40, 2525–2538, doi:10.1175/2010JPO4462.1, 2010.

Rayner, P. J., Law, R. M., Allison, C. E., Francey, R. J., Trudinger, C. M., and Pickett-Heaps, C.: Interannual variability of the global carbon cycle (1992–2005) inferred by inversion of atmospheric CO_2 and $\delta^{13}CO_2$ measurements, Global Biogeochem. Cy., 22, GB3008, doi:10.1029/2007GB003068, 2008.

Rödenbeck, C.: Estimating CO_2 sources and sinks from atmospheric mixing ratio measurements using a global inversion of atmospheric transport, Max Planck Institute for Biogeochemistry, Jena, 2005.

Rodgers, K. B., Blanke, B., Madec, G., Aumont, O., Ciais, P., and Dutay, J.-C.: Extratropical sources of Equatorial Pacific upwelling in an OGCM, Geophys. Res. Lett., 30, 1084, doi:10.1029/2002GL016003, 2003.

Rodgers, K. B., Sarmiento, J. L., Aumont, O., Crevoisier, C., de Boyer Montegut, C., and Metzl, N.: A wintertime uptake window for anthropogenic CO_2 in the North Pacific, Global Biogeochem. Cy., 22, GB2020, doi:10.1029/2006GB002920, 2008.

Schuster, U., McKinley, G. A., Bates, N., Chevallier, F., Doney, S. C., Fay, A. R., González-Dávila, M., Gruber, N., Jones, S., Krijnen, J., Landschützer, P., Lefèvre, N., Manizza, M., Mathis, J., Metzl, N., Olsen, A., Rios, A. F., Rödenbeck, C., Santana-Casiano, J. M., Takahashi, T., Wanninkhof, R., and Watson, A. J.: An assessment of the Atlantic and Arctic sea-air CO_2 fluxes, 1990–2009, Biogeosciences, 10, 607-627, doi:10.5194/bgd-9-10669-2012, 2013.

Sugimoto, H., Hiraishi, N., Ishii, M., and Midorikawa, T.: The development of the air-sea CO_2 flux estimation method in the Pacific Ocean, Tech. Rep. Meteor. Res. Inst., 66, 32 pp., 2012.

Sweeney, C., Gloor, E., Jacobson, A. R., Key, R. M., McKinley, G., Sarmiento, J. L., and Wanninkhof, R.: Constraining global air-sea gas exchange for CO_2 with recent bomb ^{14}C measurements, Global Biogeochem. Cy., 21, GB2015, doi:10.1029/2006GB002784, 2007.

Takahashi, T., Olafsson, J., Goddard, J. G., Chipman, D. W., and Sutherland, S. C.: Seasonal variation of CO_2 and nutrients in the high-latitude surface oceans: a comparative study, Global Biogeochem. Cy., 7, 843–878, doi:10.1029/93GB02263, 1993.

Takahashi T., Feely, R. A., Weiss, R., Wanninkhof, R. H., Chipman, D. W., Sutherland, S. C., and Takahashi, T.: Global air-sea flux of CO_2: An estimate based on measurements of sea-air pCO_2 difference, P. Natl. Acad. Sci., 94, 8292–8299, 1997.

Takahashi, T., Sutherland, S. C., Sweeney, C., Poisson, A., Metzl, N., Tilbrook, B., Bates, N., Wanninkhof, R., Feely, R. A., Sabine, C., Olafsson, J., and Nojiri, Y.: Global sea–air CO_2 flux based on climatological surface ocean pCO_2, and seasonal biological and temperature effects, Deep-Sea Res. II, 49, 1601–1622, 2002.

Takahashi, T., Sutherland, S. C., Feely, R. A., and Cosca, C. E.: Decadal variation of the surface water pCO_2 in the western and central equatorial Pacific, Science, 302, 852–856, doi:10.1126/science.1088570, 2003.

Takahashi, T., Sutherland, S. C., Feely, R. A., and Wanninkhof, R.: Decadal change of the surface water pCO_2 in the North Pacific: A synthesis of 35 years of observations, J. Geophys. Res., 111, C07S05, doi:10.1029/2005JC003074, 2006.

Takahashi, T., Sutherland, S. C., and Kozyr, A.: Global ocean surface water partial pressure of CO_2 database: measurements performed during 1968–2006 (Version 1.0), ORNL/CDIAC-152, NDP-088, Carbon Dioxide Information Analysis Center, Oak Ridge National Laboratory, U.S. Department of Energy, Oak Ridge, Tennessee, 20 pp., 2008.

Takahashi, T., Sutherland, S. C., Wanninkhof, R., Sweeney, C., Feely, R. A., Chipman, D. W., Hales, B., Friederich, G., Chavez, F., Sabine, C., Watson, A., Bakker, D. C. E., Schuster, U., Metzl, N., Inoue. H. Y., Ishii, M., Midorikawa, T., Nojiri, Y., Körtzinger, A., Steinhoff, T., Hoppema, M., Olafsson, J., Arnarson, T. S., Tilbrook, B., Johannessen, T., Olsen, A., Bellerby, R., Wong, C. S., Delille, B., Bates, N. R., and de Baar, H. J. W.: Climatological mean and decadal change in surface ocean pCO_2, and net sea-air CO_2 flux over the global oceans, Deep-Sea Res. II, 56, 554–577, doi:10.1016/j.dsr2.2008.12.009, 2009a.

Takahashi, T., Sutherland, S. C., and Kozyr, A.: Global ocean surface water partial pressure of CO_2 database: measurements performed during 1968–2008 (Version 2008), ORNL/CDIAC-152, NDP-088r, Carbon Dioxide Information Analysis Center, Oak Ridge National Laboratory, U.S. Department of Energy, Oak Ridge, Tennessee, doi:10.3334/CDIAC/otg.ndp088r, 2009b.

Tans, P. P., Fung, I. Y., and Takahashi, T.: Observational constrains on the global atmospheric CO_2 budget, Science, 247, 1431–1438, doi:10.1126/science.247.4949.1431, 1990.

Telszewski, M., Chazottes, A., Schuster, U., Watson, A. J., Moulin, C., Bakker, D. C. E., González-Dávila, M., Johannessen, T., Körtzinger, A., Lüger, H., Olsen, A., Omar, A., Padin, X. A., Ríos, A. F., Steinhoff, T., Santana-Casiano, M., Wallace, D. W. R., and Wanninkhof, R.: Estimating the monthly pCO_2 distribution in the North Atlantic using a self-organizing neural network, Biogeosciences, 6, 1405–1421, doi:10.5194/bg-6-1405-2009, 2009.

Tsurushima, N., Nojiri, Y., Imai, K., and Watanabe, S.: Seasonal variations of carbon dioxide system and nutrients in the surface

mixed layer at station KNOT (44° N, 155° E) in the subarctic western North Pacific, Deep-Sea Res. II, 49, 5377–5394, 2002.

Uppala, S. M., Kållberg, P. W., Simmons, A. J., Andrae, U., da Costa Bechtold, V., Fiorino, M., Gibson, J. K., Haseler, J., Hernandez, A., Kelly, G. A., Li, X., Onogi, K., Saarinen, S., Sokka, N., Allan, R. P., Andersson, E., Arpe, K., Balmaseda, M. A., Beljaars, A. C. M., van de Berg, L., Bidlot, J., Bormann, N., Caires, S., Chevallier, F., Dethof, A., Dragosavac, M., Fisher, M., Fuentes, M., Hagemann, S., Hólm, E., Hoskins, B. J., Isaksen, L., Janssen, P. A. E. M., Jenne, R., McNally, A. P., Mahfouf, J.-F., Morcrette, J. J., Rayner, N. A., Saunders, R. W., Simon, P. W., Sterl, P., Trenberth, K. E., Untch, A., Vasiljevic, D., Viterbo, P., and Woollen J.: The ERA-40 re-analysis, Quart. J. R. Meteorol. Soc., 131, 2961–3012, doi:10.1256/qj.04.176, 2005.

Valsala, V. and Maksyutov, S.: Simulation and assimilation of global ocean pCO_2 and air-sea CO_2 fluxes using ship observations of surface ocean pCO_2 in a simplified biogeochemical offline model, Tellus B, 62, 821–840, doi:10.1111/j.1600-0889.2010.00495.x, 2010.

Valsala, V., Maksyutov, S., Telszewski, M., Nakaoka, S., Nojiri, Y., Ikeda, M., and Murtugudde, R.: Climate impacts on the structures of the North Pacific air-sea CO_2 flux variability, Biogeosciences, 9, 477–492, doi:10.5194/bg-9-477-2012, 2012.

Wang, X., Christian, J. R., Murtugudde, R., and Busalacchi, A. J.: Spatial and temporal variability of the surface water pCO_2 and air-sea CO_2 flux in the equatorial Pacific during 1980–2003: A basin-scale carbon cycle model, J. Geophys. Res., 111, C07S04, doi:10.1029/2005JC002972, 2006.

Wannikhof, R.: Relationship between wind speed and gas exchange over the ocean, J. Geophys. Res., 97, 7373–7382, doi:10.1029/92JC00188, 1992.

Wanninkhof, R., Park, G.-H., Takahashi, T., Sweeney, C., Feely, R., Nojiri, Y., Gruber, N., Doney, S. C., McKinley, G. A., Lenton, A., Le Quéré, C., Heinze, C., Schwinger, J., Graven, H., and Khatiwala, S.: Global ocean carbon uptake: magnitude, variability and trends, Biogeosciences, 10, 1983–2000, doi:10.5194/bg-10-1983-2013, 2013.